Where Did Half of the Sun's Oxygen Go?

Testing StellarAtmosphere Models for the Sun and Other Stars with Interferometry

Jason Aufdenberg

Michelson Postdoctoral Fellow
National Optical Astronomy Observatory
Tucson, USA

$$
\begin{aligned}
\gamma(\mu+\beta)\frac{\partial I}{\partial r} \quad & +\frac{\partial}{\partial \mu}\left\{\gamma(1-\mu^2)\left[\frac{(1+\beta\mu)}{r}-\gamma^2(\mu+\beta)\frac{\partial\beta}{\partial r}\right] I\right\} \\
& -\frac{\partial}{\partial \nu}\left\{\gamma\left[\frac{\beta(1-\mu^2)}{r}+\gamma^2\mu(\mu+\beta)\frac{\partial\beta}{\partial r}\right]\nu I\right\} \\
& +\gamma\left\{\frac{2\mu+\beta(3-\mu^2)}{r}+\gamma^2(1+\mu^2+2\beta\mu)\frac{\partial\beta}{\partial r}\right\} I \\
& = \eta-\chi I.
\end{aligned}
$$

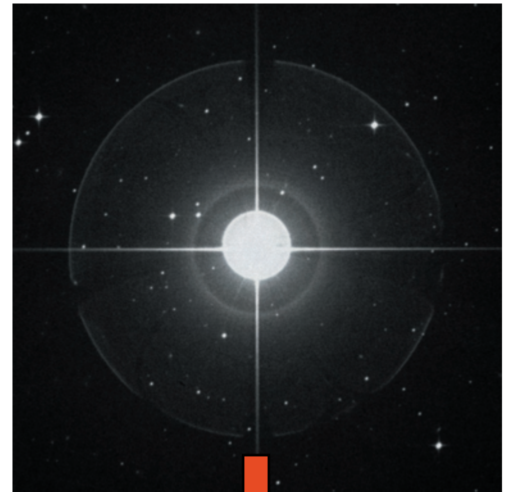

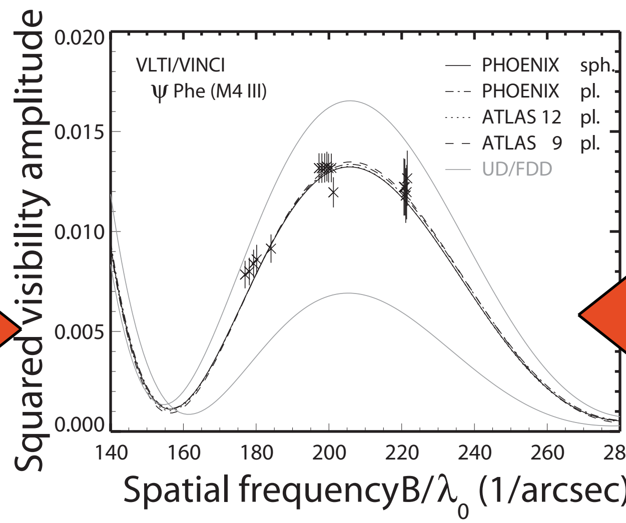

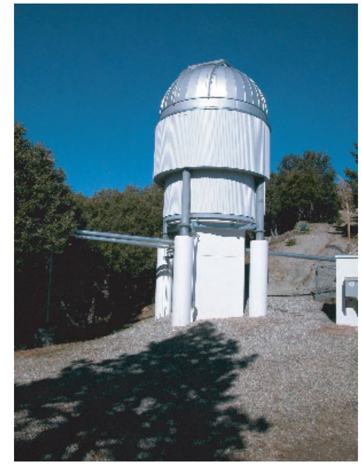

Interferometry Collaborators

S. T. Ridgway (NOAO, LESIA, Observatorie de Paris-Meduon)

P. Kervella, A. Mérand, V. Coudé du Foresto

(LESIA, Observatorie de Paris-Meduon)

D. Mozurkewich (Seabrook Engineering)

CHARA Team (Georgia State University)

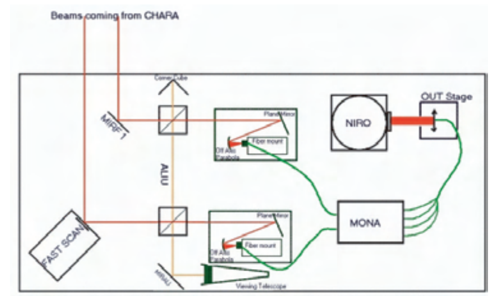

Model Atmosphere Collaborators

H.-G. Ludwig (Lund Observatory)

R. Kurucz (Smithsonian Astrophysical Observatory)

P. Hauschildt, A. Schweitzer (Hamburger Sternwarte)

F. Allard (CRAL-ENS, Lyon)

E. Baron (University of Oklahoma)

T. Barman (Wichita State University)

C. I. Short (St. Mary's University)

```
      program phoenix
c     ---------------
c--
c-- used modules:
c--
      use phoenix_variables
      use phx_interfaces, dummy_takeband =>
      implicit none
*******************************
*              the main program for phoenix
```

What's to Come....

Intro: All about limb darkening

Part I: Procyon, Convection, and Limb Darkening

Part II: Deneb, Stellar Winds, and Limb Darkening

Limb Darkening Basics

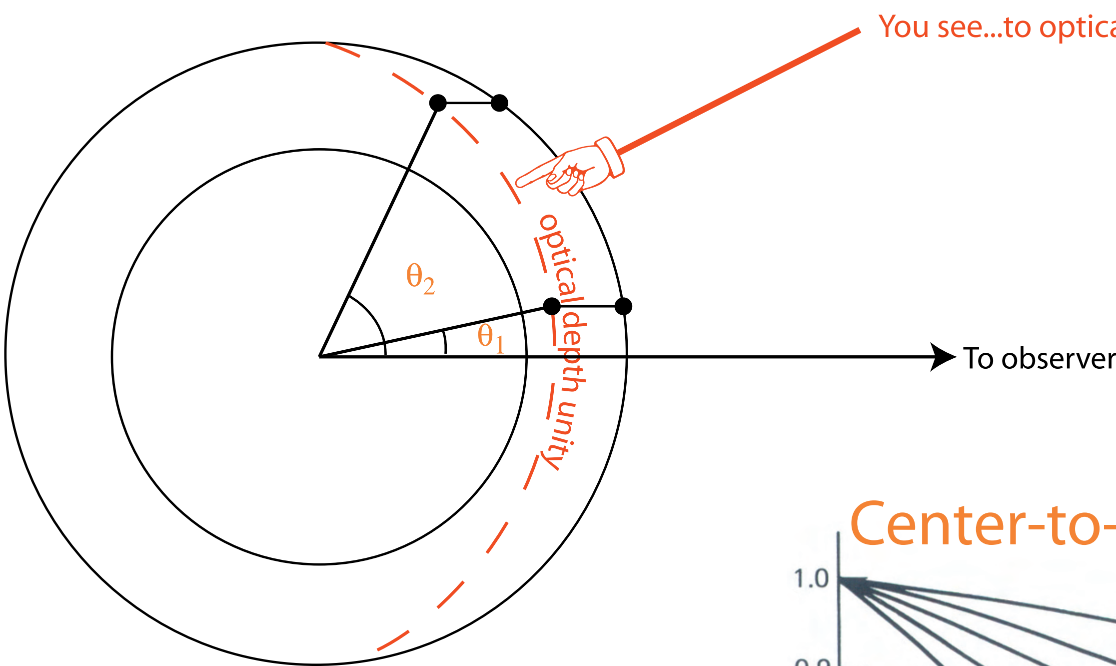

$$B_\lambda = 2\,ckT\ \lambda^{-4}$$

$$\frac{dB_\lambda}{dT} = \frac{2}{c}k\ \lambda^{-4}$$

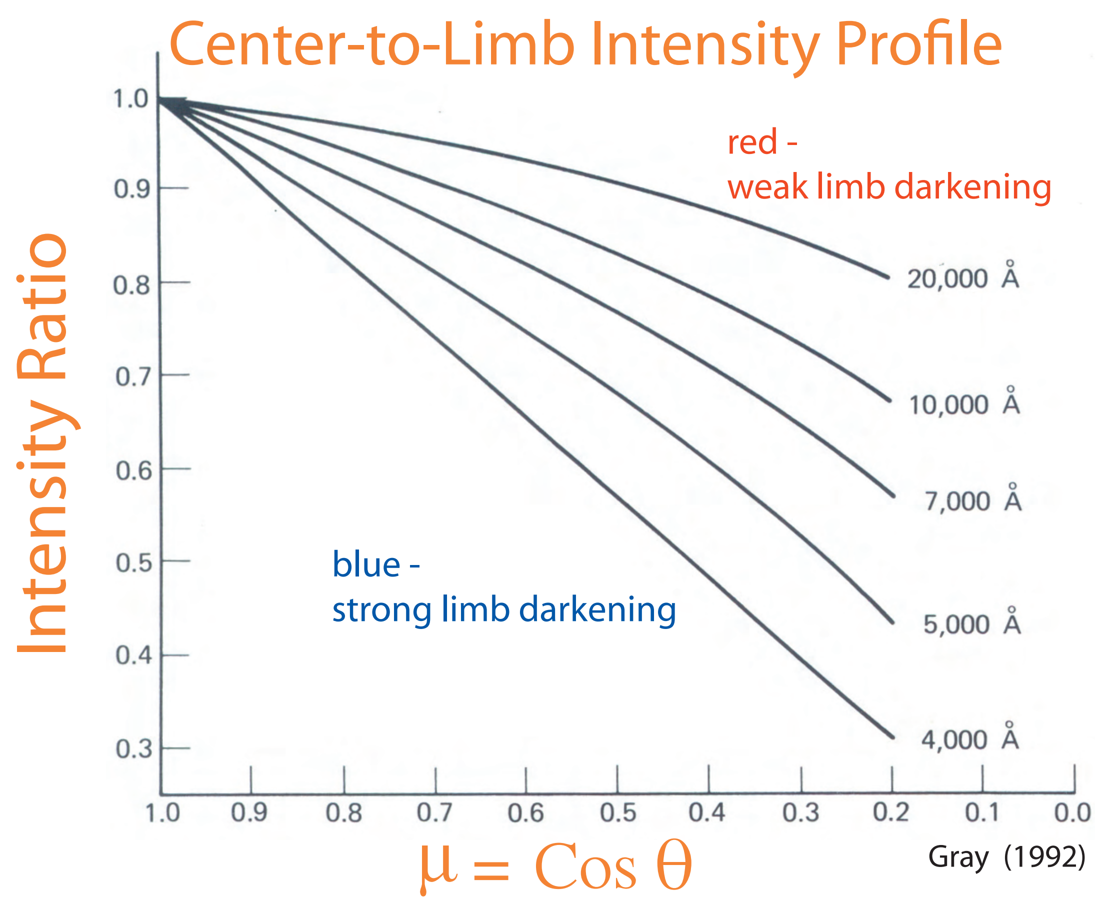

Gray (1992)

Early Multi-Wavelength Limb Darkening

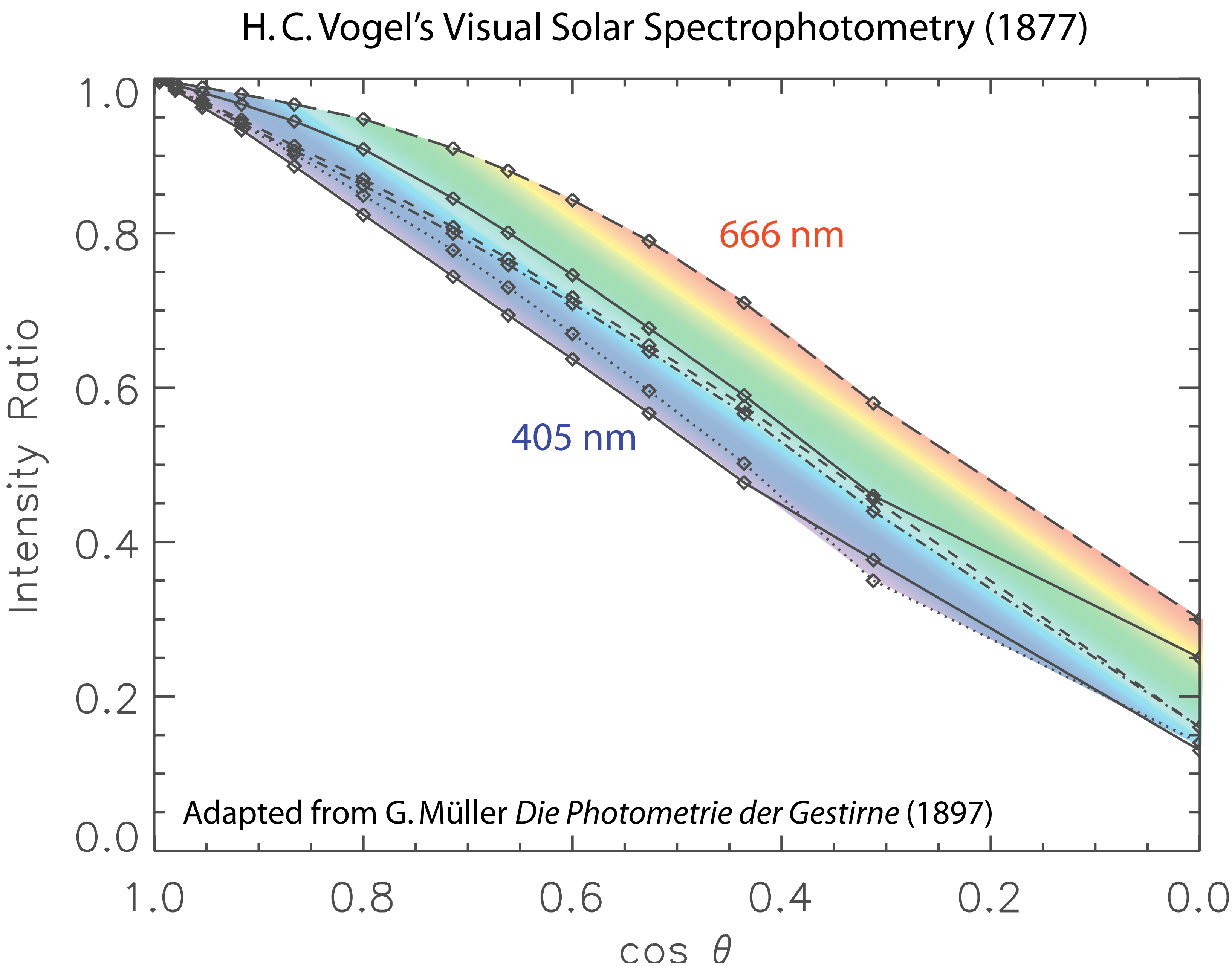

Early Model Limb Darkening Models

1906 - K. Schwarzschild
Derived a center-to-limb profile for the Sun with a radiative equilibrium temperature structure. He showed this to be consistent with observations, ruling out an adiabatic equilibrium temperature structure.

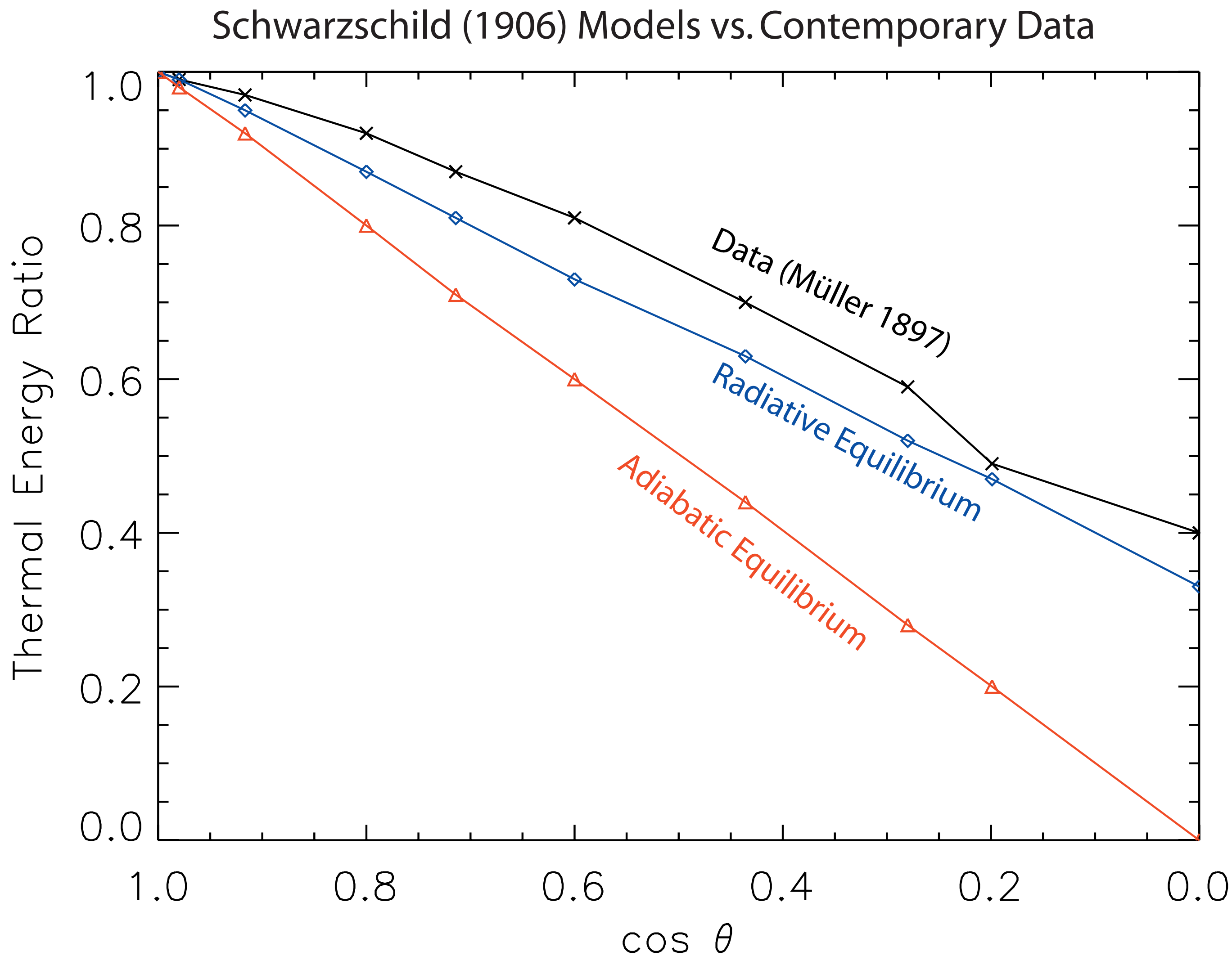

Adapted from K. Schwarzschild (1906) "Über das Gleichgewicht der Sonnenatmosphäre"
Nachrichten von der Königlichen Gesellschaft der Wissenschaften zu Göttingen. Math.-phys. Kalsse, 295, 41
Translation in D. H. Menzel, Ed., *Selected Papers on the Transfer of Radiation* (1966) NY: Dover

Assumptions: mass absorption coefficent is both wavelength and depth independent. Angular-dependent intensity is replaced by its mean.

New Models, New Physics, Hydrogen and the Origins of Convective Instability

1921 - E. A. Milne
Replaced Schwarzchild's mean intensity by an angular average producing a radiative equilibrium temperature structure with better flux conservation, yielding a limb darkening coefficent of in better agreement with observations.

1925 - C. Payne and H. N. Russell
Established hydrogen as the principal component of the solar atmosphere.

1930 - A. Unsöld
Investigated the effects of hydrogen ionization on the stability of radiative equilibrium against convection.

1939 - R. Wildt
Recognizes the importance of wavelength dependent H^- bound-free and free-free opacity. This opacity causes the solar atmosphere to be unstable to convection.

Wavelength-Dependent Opacity of the Solar Atmosphere

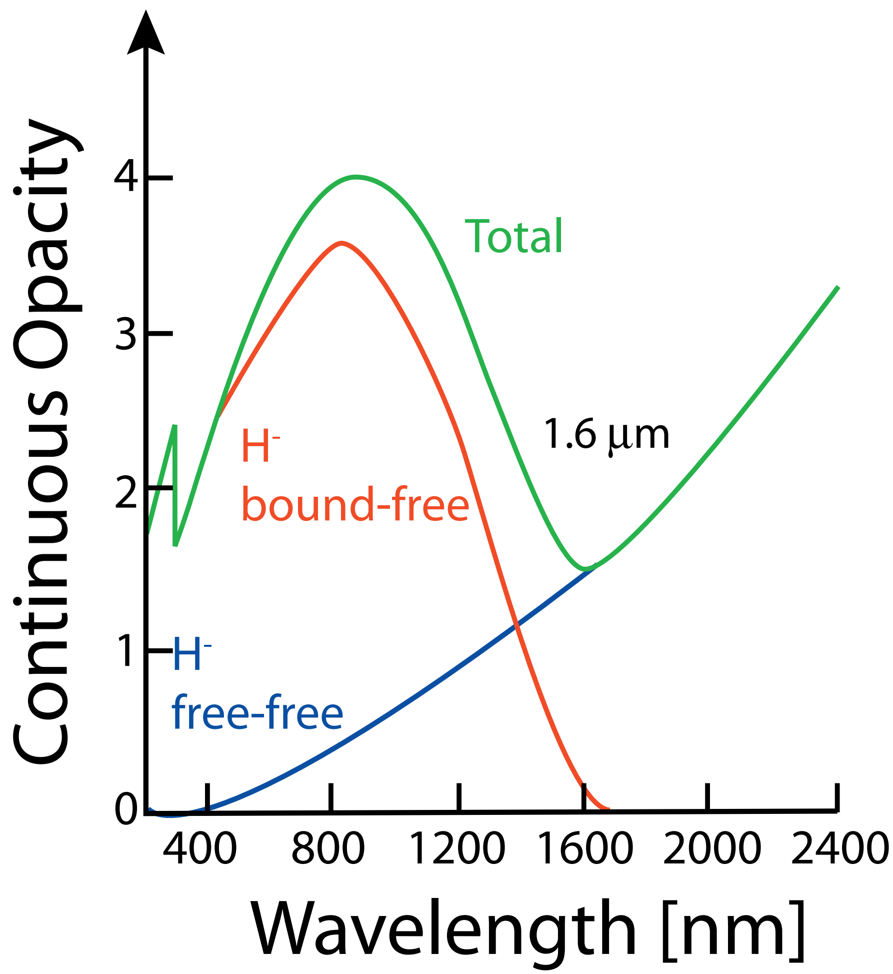

Reconstructing the Sun's Temperature Structure by Inverting the Planck Function

$$T_b^{\text{center}} = \frac{14388}{\lambda \ln [(11909/\lambda^5 I_\lambda) + 1]}$$

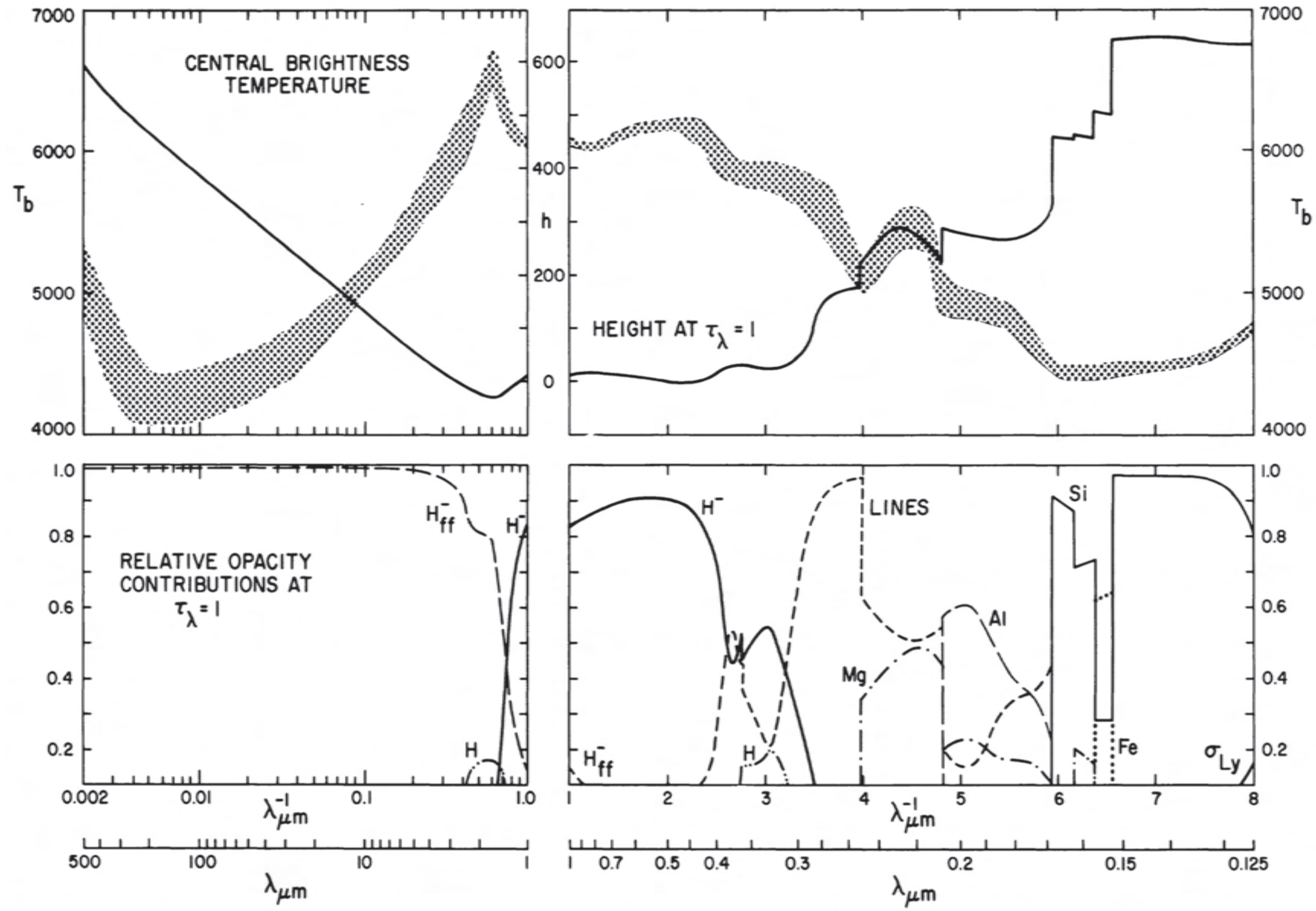

Vernezza, Avrett, & Loeser (1976) ApJS 30, 1

Linking Intensity to Depth: The Eddington-Barbier Approximation

$$I_\nu^+(\tau_\nu = 0, \mu) = \int_0^\infty S_\nu(t_\nu)\, \mathrm{e}^{-t_\nu/\mu}\, \mathrm{d}t_\nu/\mu.$$

$$I_\nu^+(\tau_\nu = 0, \mu) \;\approx\; S_\nu(\tau_\nu = \mu)$$

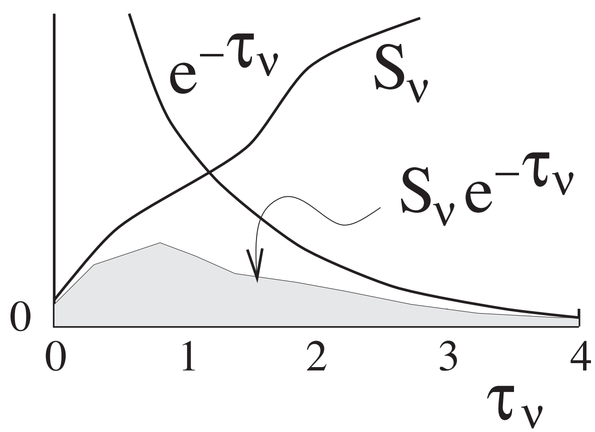

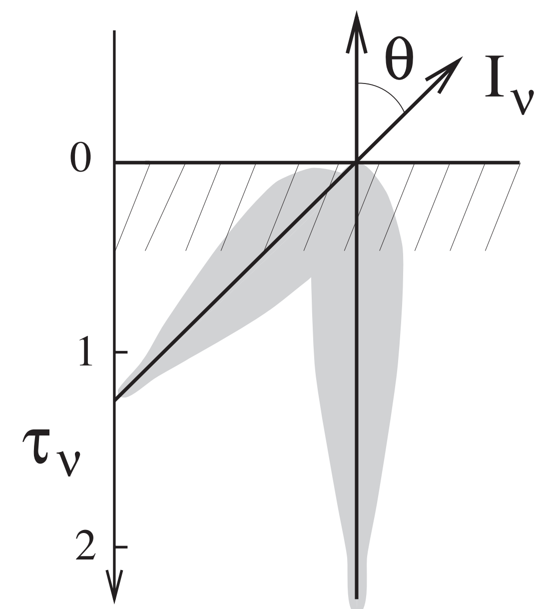

From Rob Rutten's excellent lecture notes:
http://www.phys.uu.nl/~rutten/Astronomy_lecture.html

Solar Limb Darkening and the Overshooting Approximation

Castelli, Gratton & Kurucz (1997) A&A 318, 841

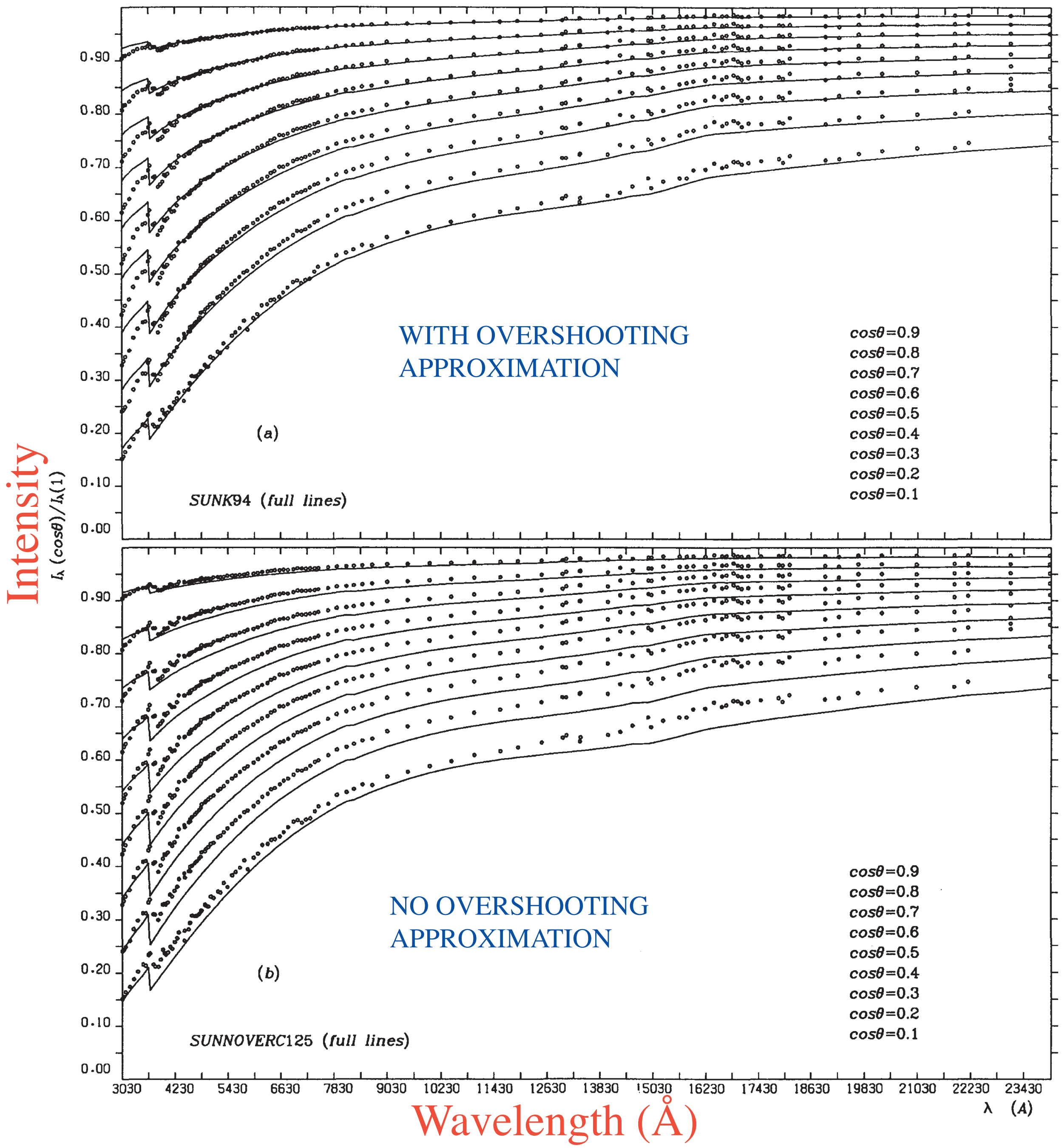

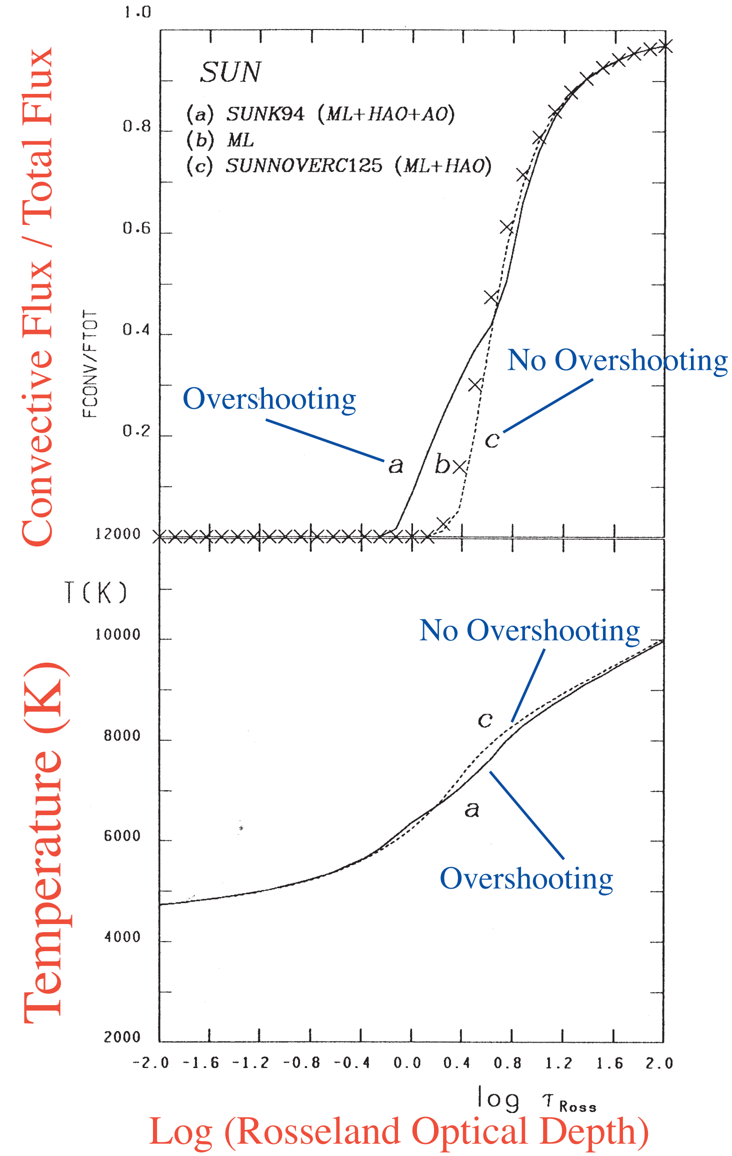

Multi-Wavelength Diameters from Speckle Interferometry (@Palomar)

Alpha Ori
~50 milli-arcseconds

Alpha Lyr
~3 milli-arcseconds

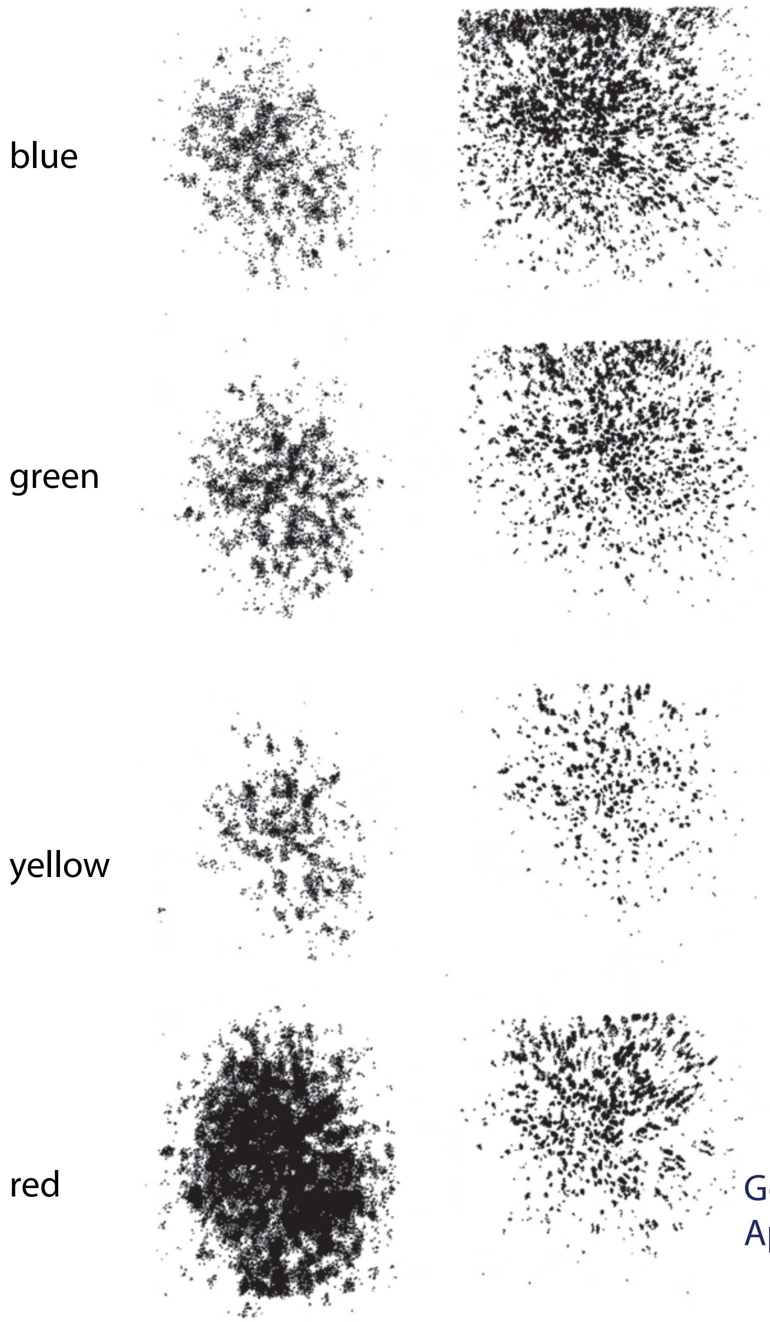

Gezari et al. (1972)
ApJ, 173, L1

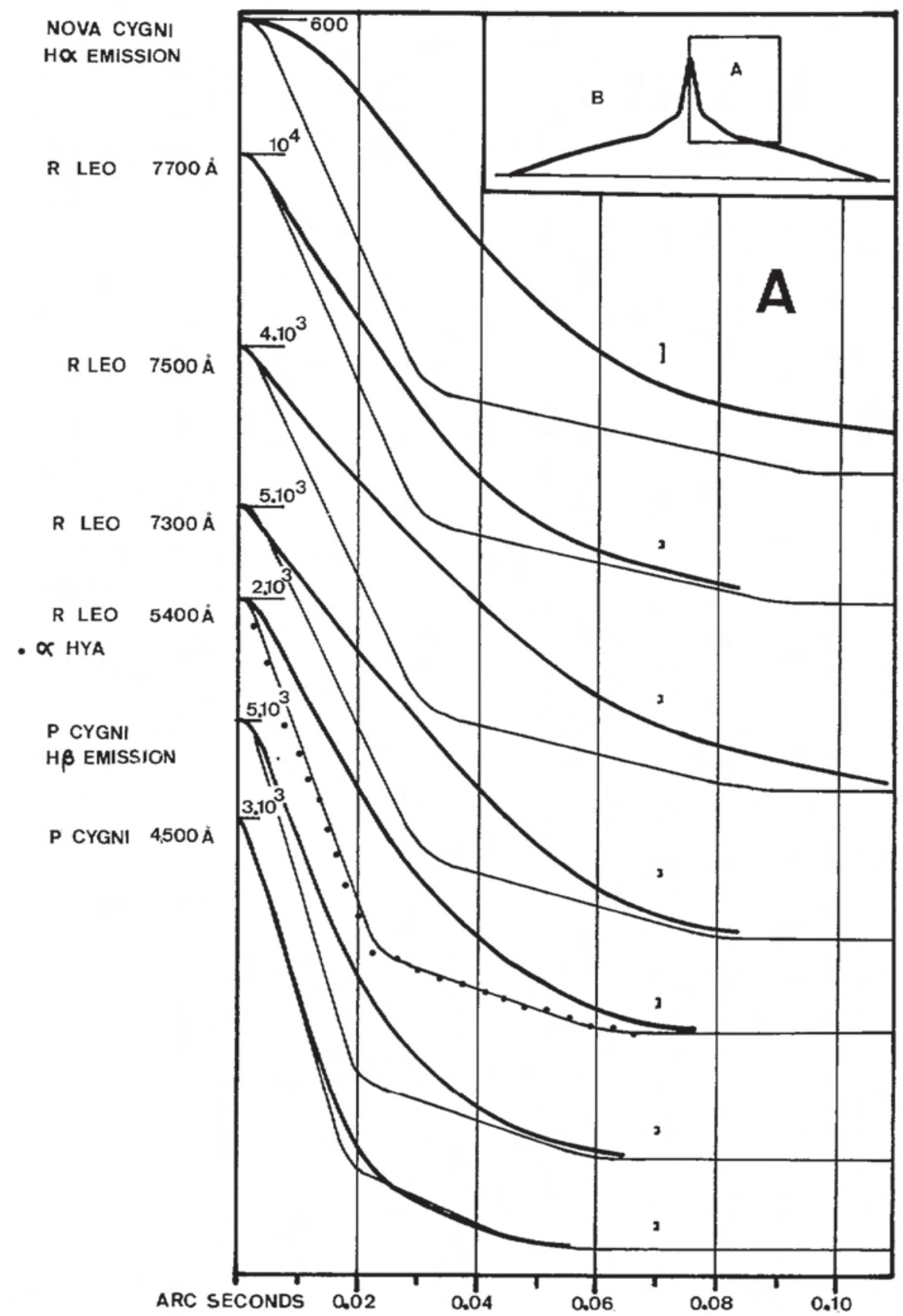

Blazit et al. (1977)
ApJ, 214, L79

Limb-Darkening Measurements from Lunar Occultation

Ridgway *et al.* (1982)
AJ 87, 104

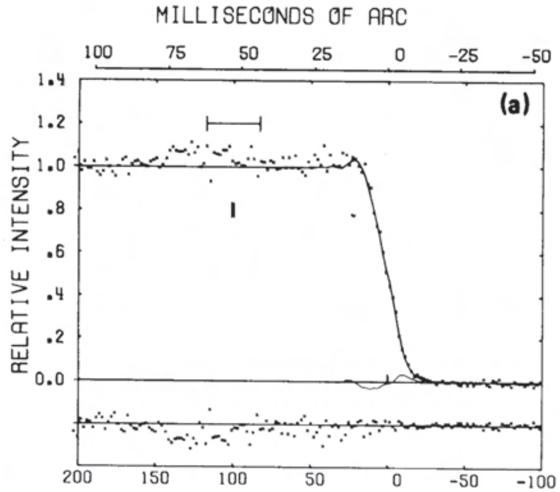

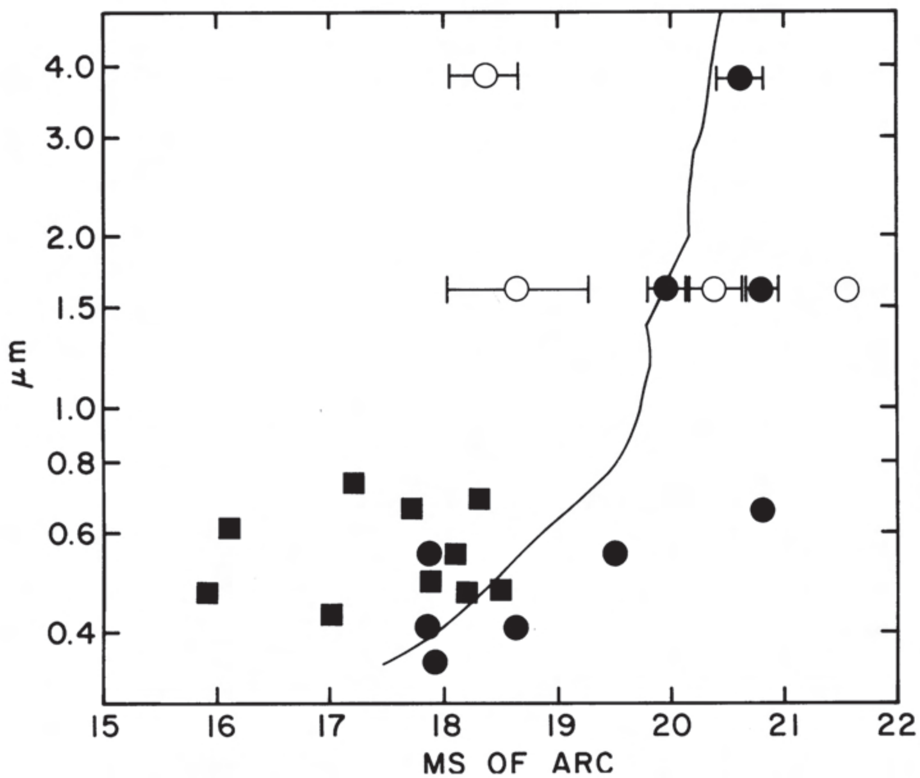

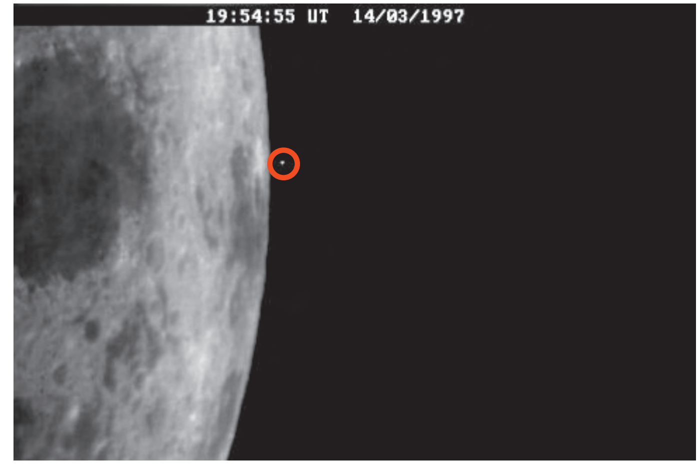

Worth Hill Observatory

Delaware Valley Amateur Astronomers

Limb Darkening Measurements from Microlensing

Abe et al. (2003) A&A 411, L493

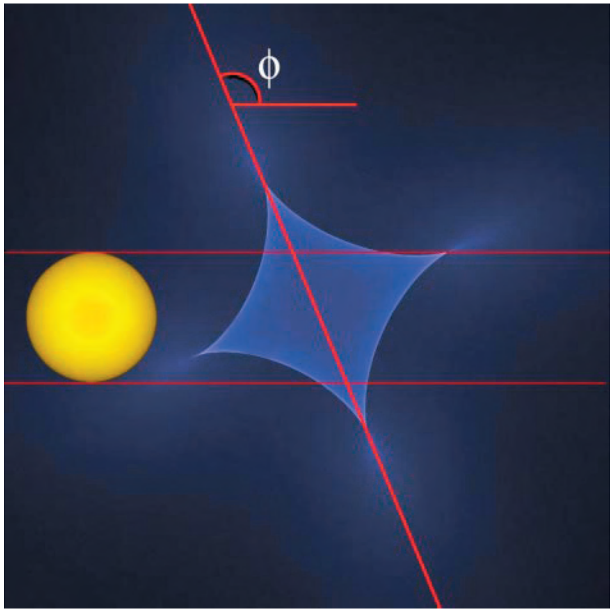

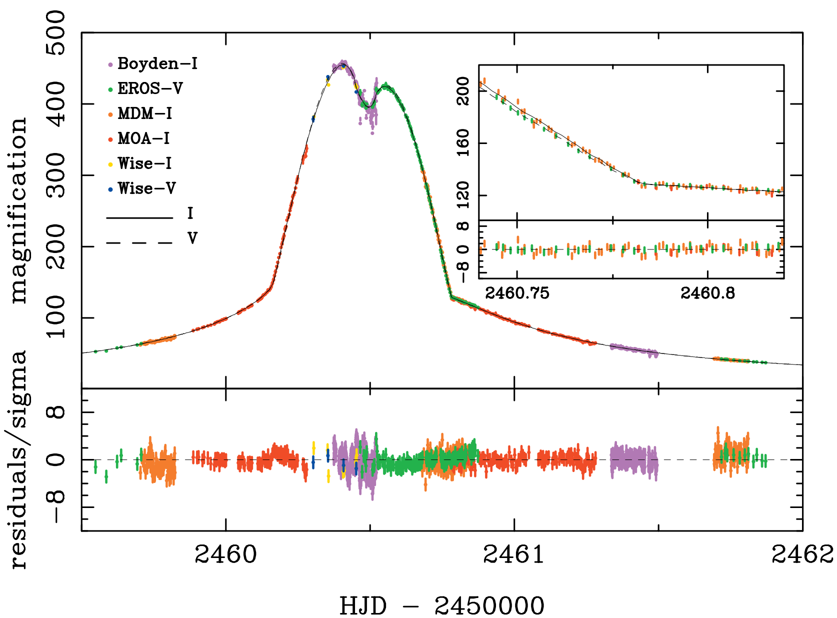

Fields et al. (2003) ApJ 596, 1305

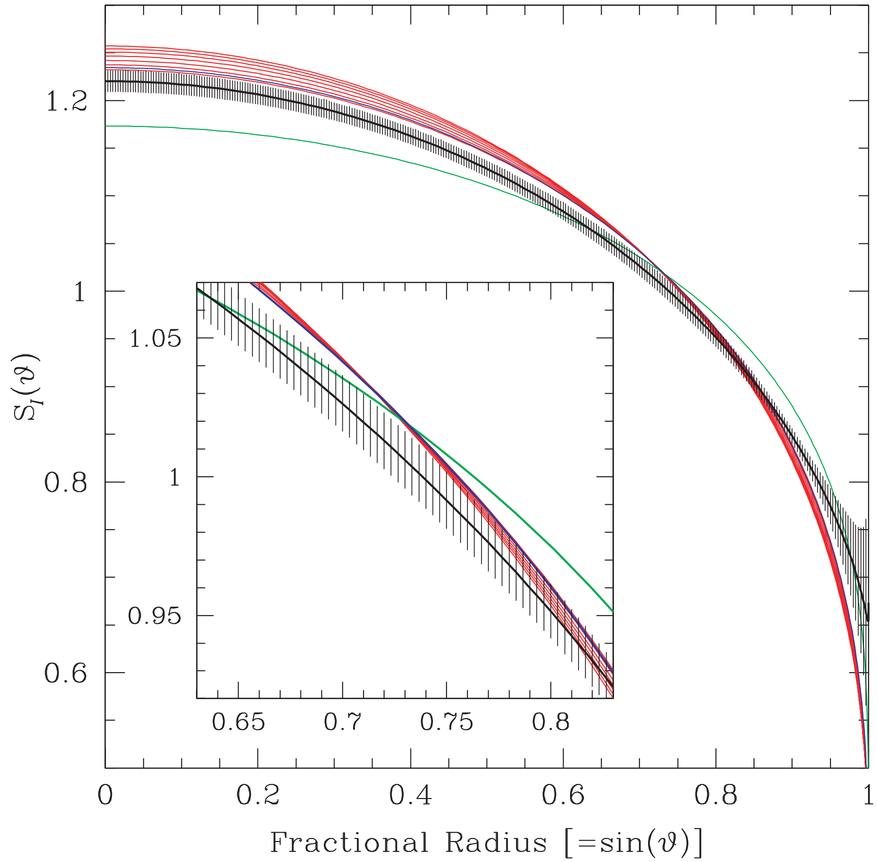


VLTI Chile
SUSI Australia
CHARA California
GI2T France
Keck Hawaii
Interferometer Laboratory
(South) Observing House
Center Room
(North) Observing House
30m
MIRA Japan
COAST England
IOTA Arizona
ISI California
NPOI Arizona

Schematic Two-Telescope Interferometer

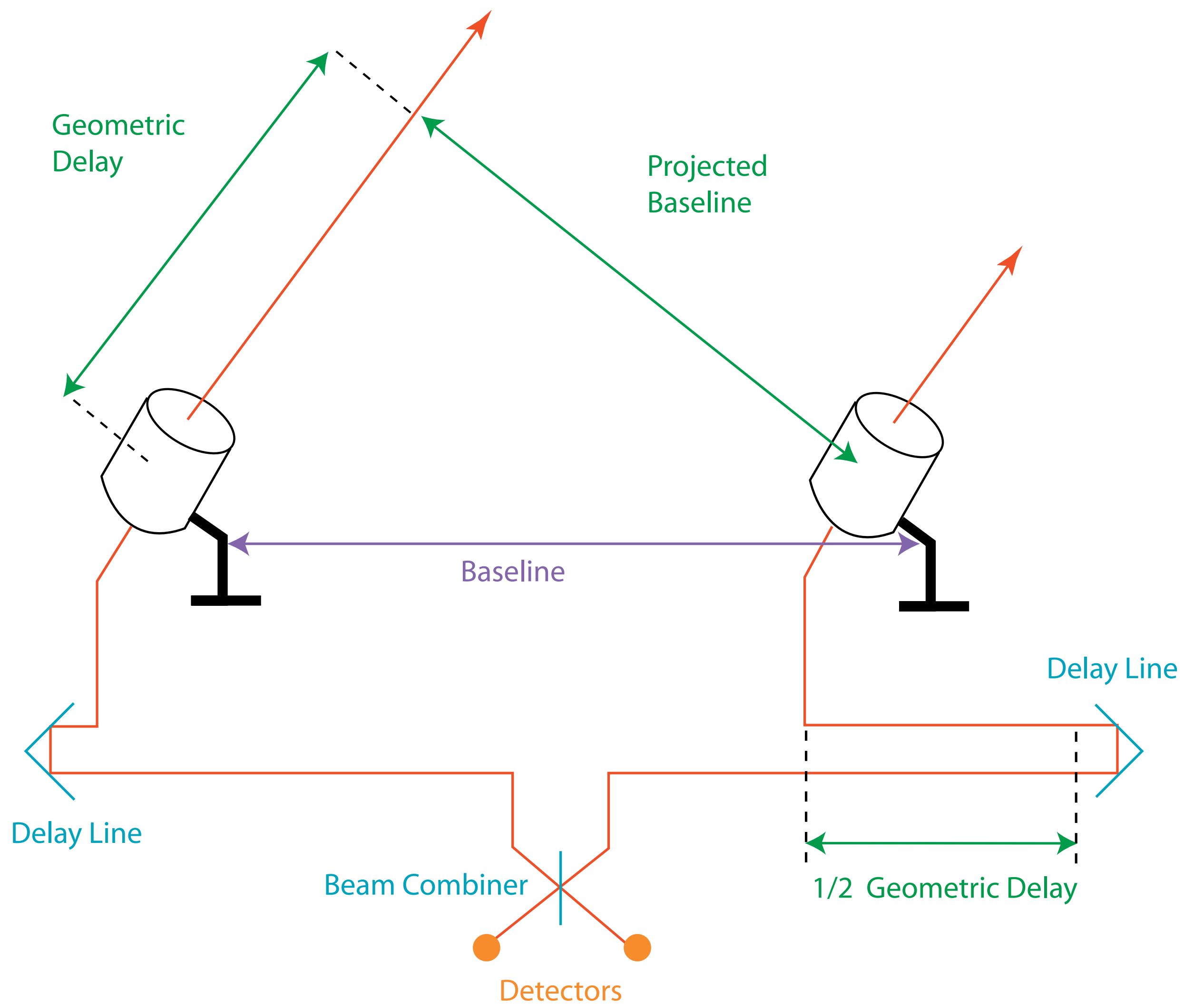

adapted from Oskar van der Lühe

The Observable: Visibility

$$V = \frac{I_{max} - I_{min}}{I_{max} + I_{min}}$$

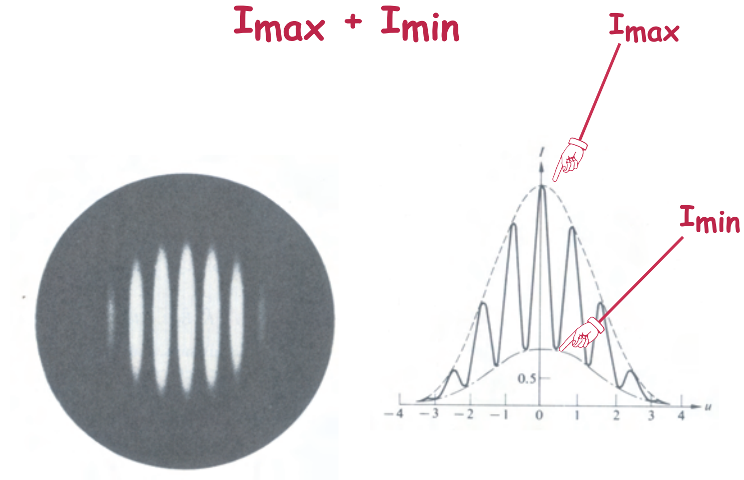

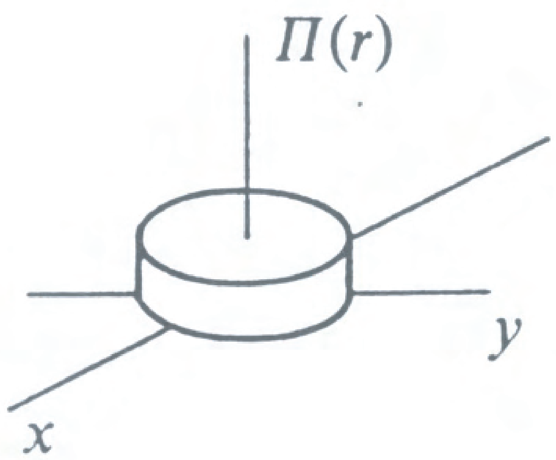

on the sky

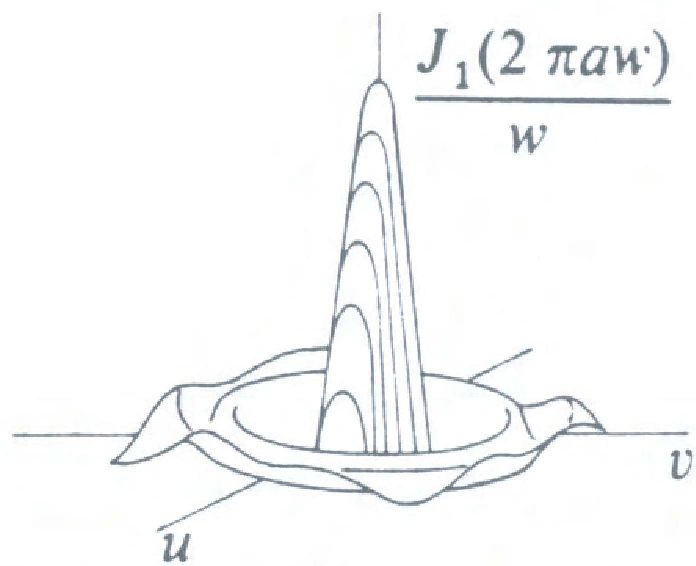

what the interferometer measures

"Direct" Limb darkening measurements from interferometry

- **M5 II** α Her (Perrin et al., 2004)
- **M4.5 III** BY Boo (Wittkowski et al., 2001)
- **M4 III** V416 Lac, ψ Phe (Wittkowski et al., 2001; Wittkowski et
- **M1Iab** Betelgeuse (a Ori; Burns et al., 1997; Perrin et al., 2004)
- **M0 III** γ Sge (Wittkowski et al., 2001)
- **K2 III** α Ari (Hajian et al., 1998)
- **K1.5 III** Arcturus (α Boo; Quirrenbach et al., 1996)
- **K0 III** α Cas (Hajian et al., 1998)
- **A7 V** α Aql (Ohishi et al., 2004)
- **A1 V** Sirius (α CMa; Hanbury Brown et al., 1974)

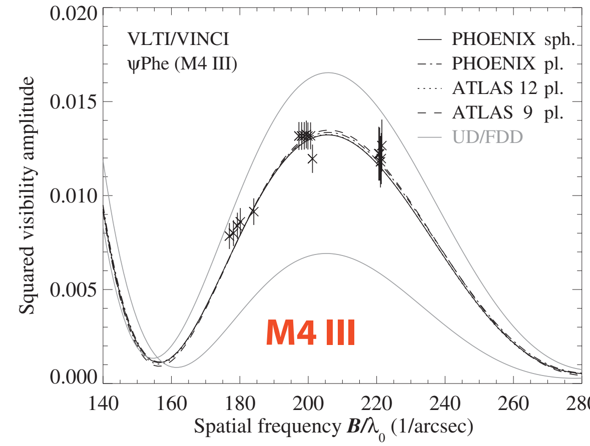

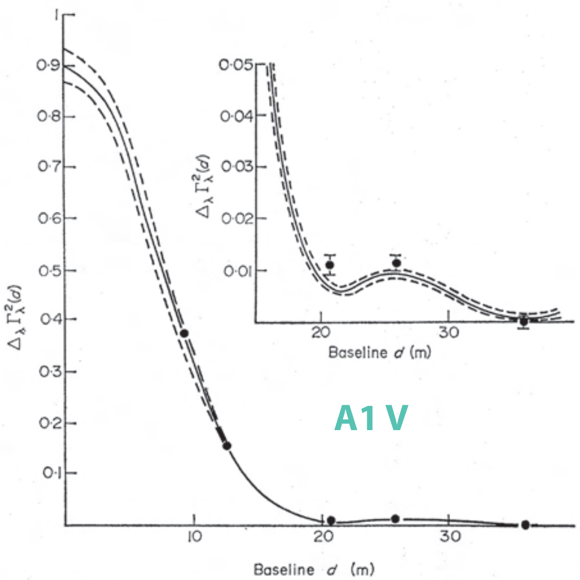

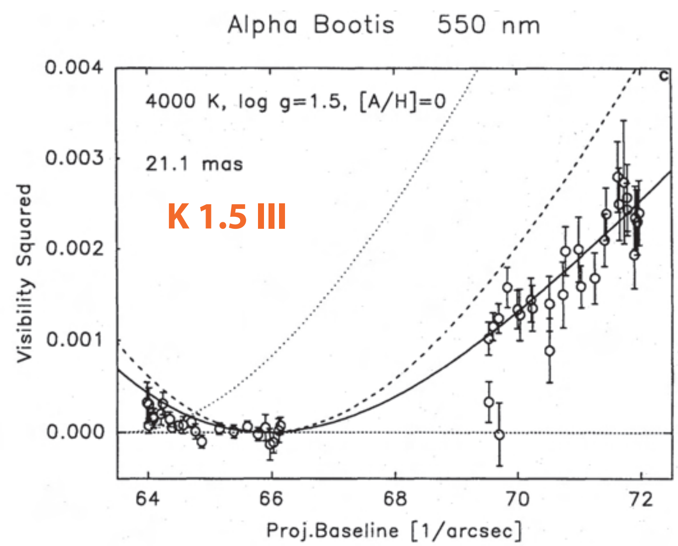

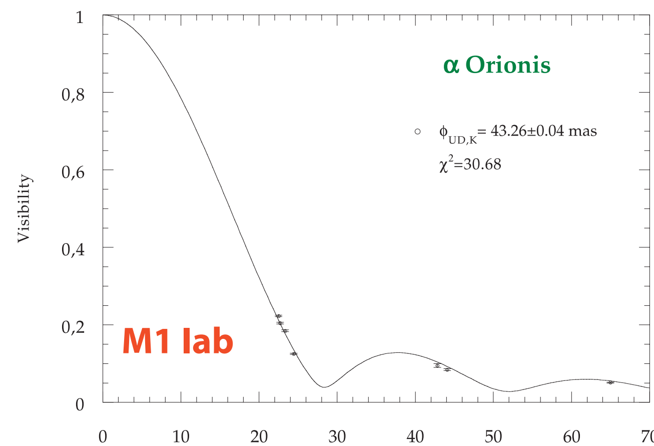

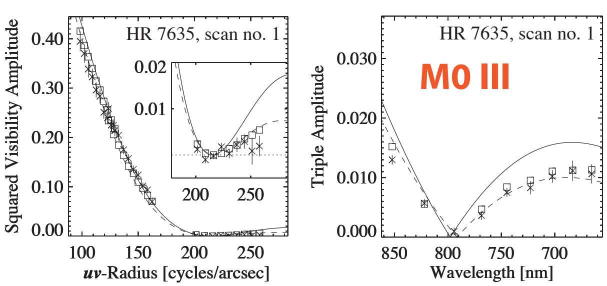

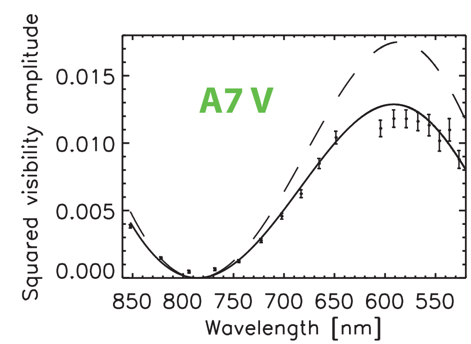

New Direct Limb Darkening Measurements
B- and A-type Supergiants & F-type stars

M5 II
M4.5 III
M4 III
M1Iab
M0 III
K2 III
K1.5 III
K0 III
F7 Ib Polaris
F5 IV Procyon ←
F2 III β Cas
A7 V
A2 Ia Deneb ←
A1 V
B8 Ia Rigel ←

Part I

Procyon, Convection, and Limb Darkening

A&A 417, 751–768 (2004)
DOI: 10.1051/0004-6361:20034328

Astronomy & Astrophysics

Asplund et al. (2004) A&A 417, 751

Recent 3-D radiative transfer models have reduced the solar oxygen abundance by nearly a factor of 2!

Line formation in solar granulation

IV. [O I], O I and OH lines and the photospheric O abundance

M. Asplund[1], N. Grevesse[2,3], A. J. Sauval[4], C. Allende Prieto[5], and D. Kiselman[6]

[1] Research School of Astronomy and Astrophysics, Mt. Stromlo Observatory, Cotter Rd., Weston, ACT 2611, Australia
[2] Centre Spatial de Liège, Université de Liège, avenue Pré Aily, 4031 Angleur-Liège, Belgium
[3] Institut d'Astrophysique et de Géophysique, Université de Liège, Allée du 6 août, 17, B5C, 4000 Liège, Belgium
[4] Observatoire Royal de Belgique, avenue circulaire, 3, 1180 Bruxelles, Belgium
[5] McDonald Observatory and Department of Astronomy, University of Texas, Austin, TX 78712-1083, USA
[6] The Institute for Solar Physics of the Royal Swedish Academy of Sciences, AlbaNova University Centre, 106 91 Stockholm, Sweden

Received 17 September 2003 / Accepted 2 December 2003

Abstract. The solar photospheric oxygen abundance has been determined from [O I], O I, OH vibration-rotation and OH pure rotation lines by means of a realistic time-dependent, 3D, hydrodynamical model of the solar atmosphere. In the case of the O I lines, 3D non-LTE calculations have been performed, revealing significant departures from LTE as a result of photon losses in the lines. We derive a solar oxygen abundance of $\log \epsilon_O = 8.66 \pm 0.05$. All oxygen diagnostics yield highly consistent abundances, in sharp contrast with the results of classical 1D model atmospheres. This low value is in good agreement with measurements of the local interstellar medium and nearby B stars. This low abundance is also supported by the excellent correspondence between lines of very different line formation sensitivities, and between the observed and predicted line shapes and center-to-limb variations. Together with the corresponding down-ward revisions of the solar carbon, nitrogen and neon abundances, the resulting significant decrease in solar metal mass fraction to $Z = 0.0126$ can, however, potentially spoil the impressive agreement between predicted and observed sound speed in the solar interior determined from helioseismology.

Key words. convection – line: formation – Sun: abundances – Sun: granulation – Sun: photosphere

We derive a solar oxygen abundance of $\log \epsilon_O = 8.66 \pm 0.05$.

1. Introduction

Oxygen is the most abundant element in the Universe with a non-Big Bang nucleosynthesis origin. As a consequence, oxygen plays a central role in many different fields of astrophysics ranging from supernova physics and galaxy evolution to dating stars and production of the light elements through cosmic ray spallation. Yet it appears that in many crucial objects for which accurate knowledge of the oxygen abundances is necessary the oxygen content is hotly debated. Recent disputes revolve around the overabundance of oxygen in metal-poor halo stars (see Asplund & García Pérez 2001; Nissen et al. 2002, and references therein), the Galactic radial abundance gradient (Rolleston et al. 2000; Cunha & Daflon 2003), and, astonishingly, the solar oxygen abundance. Partly these disagreements stem from differences in the adopted input data (e.g. gf-values, effective temperatures $T_{\rm eff}$, surface gravities $\log g$) but more importantly they reflect the choice of spectral lines to derive the abundances using classical 1D stellar model atmospheres. In particular in the solar case, the freedom of parameters to obtain consistency is very restricted yet the discrepancy is present in full.

Until recently the commonly adopted solar oxygen abundance was $\log \epsilon_O = 8.93 \pm 0.04$[1] (Anders & Grevesse 1989). This historically high abundance was suggested by analyses of the forbidden [O I] 630.0 nm line (Lambert 1978) as well as OH vibration-rotation and pure rotation lines in the infrared (Grevesse et al. 1984; Sauval et al. 1984) using the 1D hydrostatic Holweger-Müller (1974) semi-empirical model of the solar atmosphere and LTE line formation. On the other hand, a much lower abundance is indicated by the permitted high-excitation O I lines, most noteworthy the IR triplet at 777 nm, when employing the same model atmosphere with non-LTE line formation. This discrepancy of about 0.2 dex between different abundance indicators have often been blamed on over-estimated departures from local thermodynamic

Send offprint requests to: M. Asplund,
e-mail: `martin@mso.anu.edu.au`

[1] On the customary abundance scale defined as $\epsilon(X) = 10^{12} \times N(X)/N(H)$.

Until recently the commonly adopted solar oxygen abundance was $\log \epsilon_O = 8.93 \pm 0.04$[1] (Anders & Grevesse 1989).

Procyon: The Visual Binary (P = 40.82 yr)

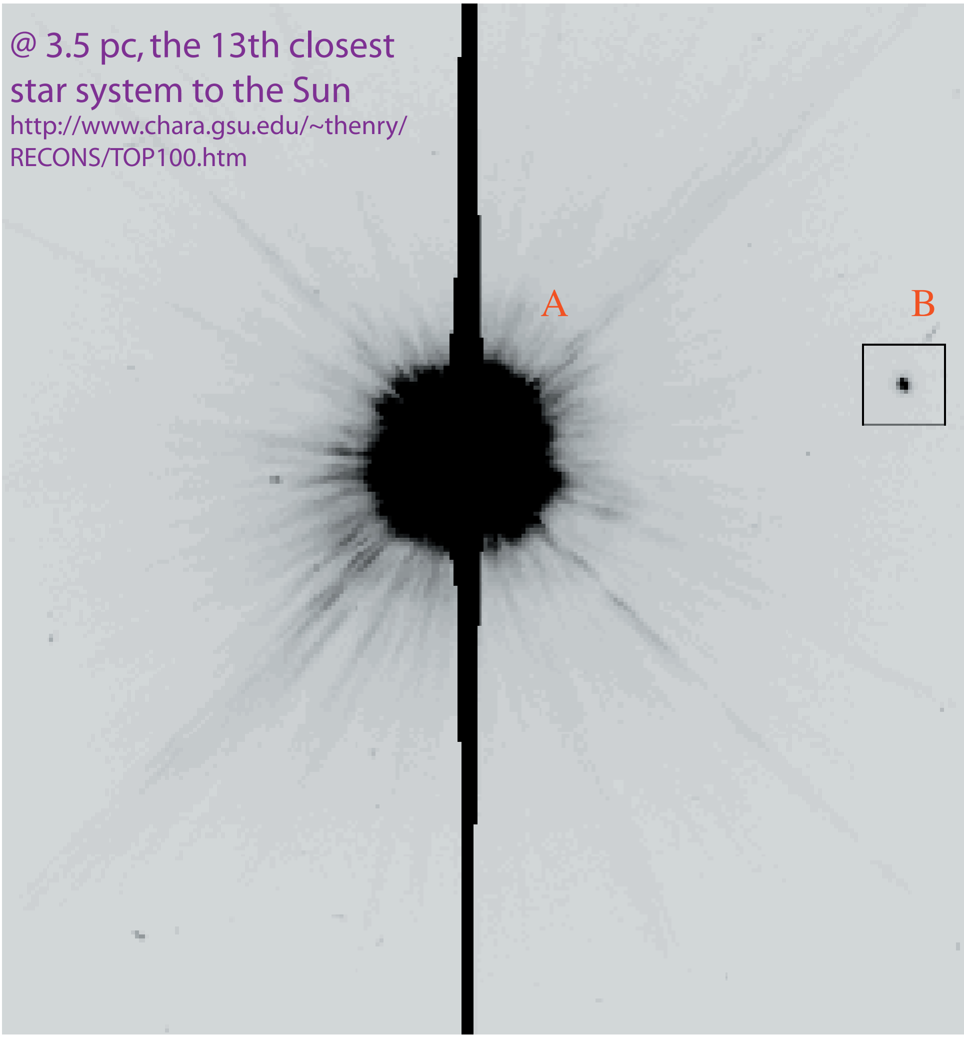

Girard et al (2000) ApJ 119, 2428

HST/WFPC2 PC image (160 s)
F218W filter

Girard et al (2000) ApJ 119, 2428

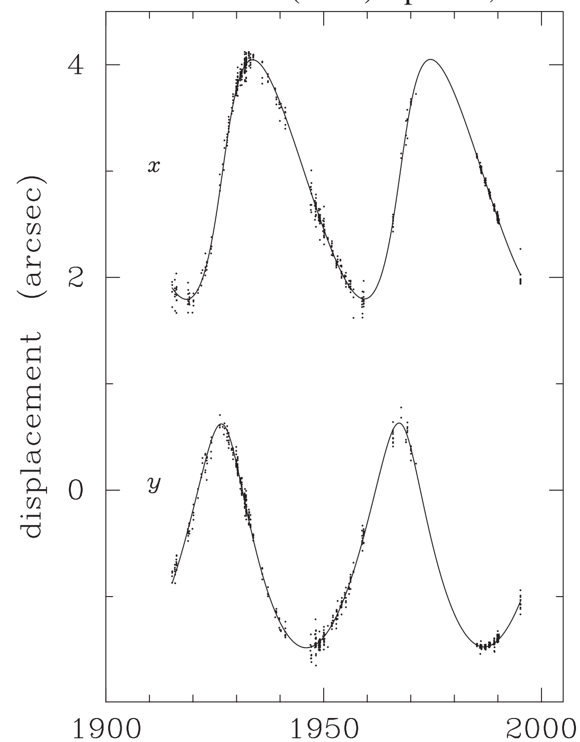

$\text{Mass}_A = 1.497 \pm 0.037\ M_\odot$
$\text{Mass}_B = 0.602 \pm 0.015\ M_\odot$

Procyon A (F5 IV): Fundamental Parameters
Angular diameter = 5.45 ± 0.05 mas (Kervella et al. 2003)
Parallax = 285.93 ± 0.88 mas (Hipparcos: Perryman et al.)
Radius = $2.05 \pm 0.02\ R_\odot$
Log(g) = 3.95 ± 0.02 cgs
Bolometric flux = $17.8 \pm 0.9 \times 10^{-9}$ W m^{-2}
Effective Temperature = 6516 ±87 K

Procyon: Astroseismology Target

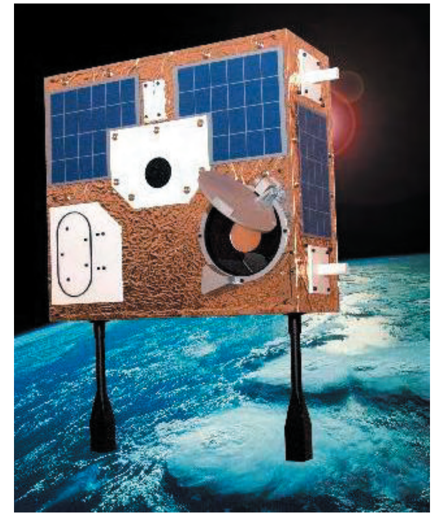

letters to nature NATURE | VOL 430 | 1 JULY 2004 |

No stellar p-mode oscillations in space-based photometry of Procyon

Jaymie M. Matthews[1], Rainer Kusching[1], David B. Guenther[2], Gordon A. H. Walker[1], Anthony F.J. Moffat[3], Slavek M. Rucinski[4], Dimitar Sasselov[5] & Werner W. Weiss[6]

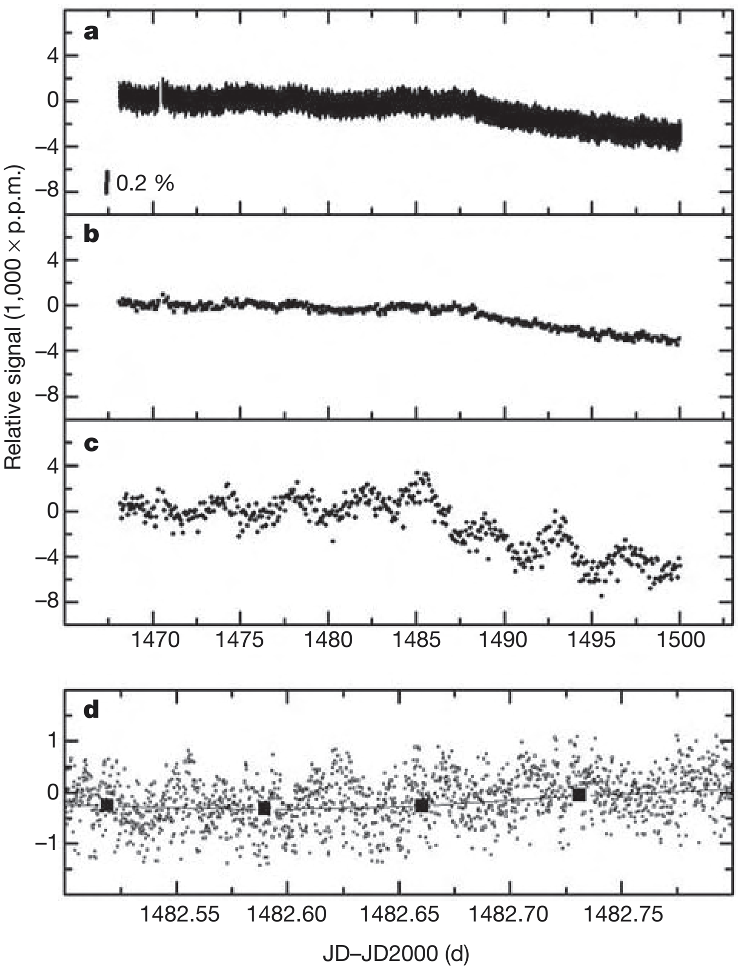

1. 32 days, 99% temporal coverage
2. p-mode peak amplitude < 15 parts per million or lifetimes less than 2-3 days

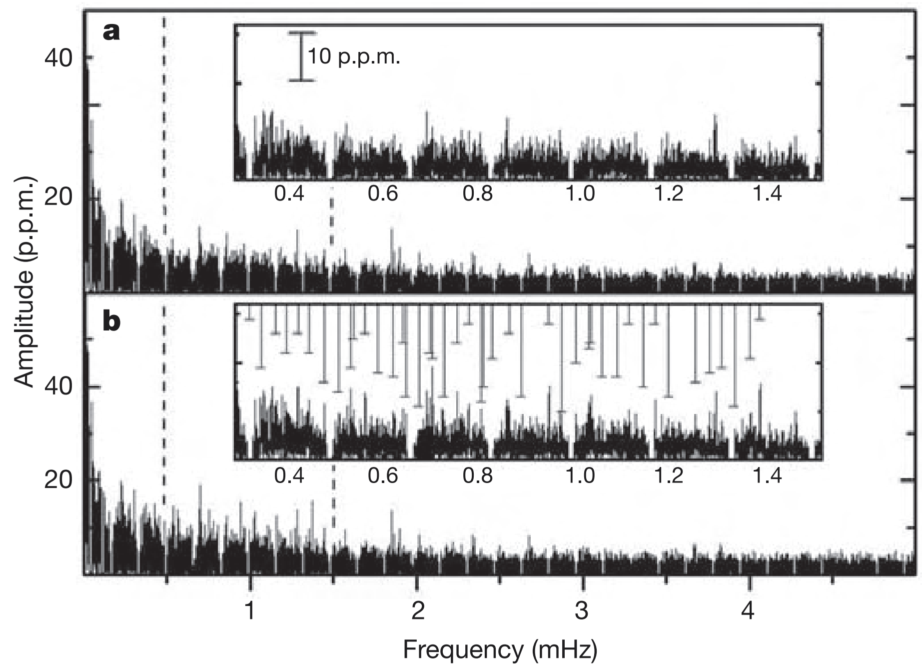

3-D Hydrodynamical Simulations of Procyon

Allende Prieto et al (2002) ApJ 567, 544

CONVECTION IN SPECTRUM OF PROCYON

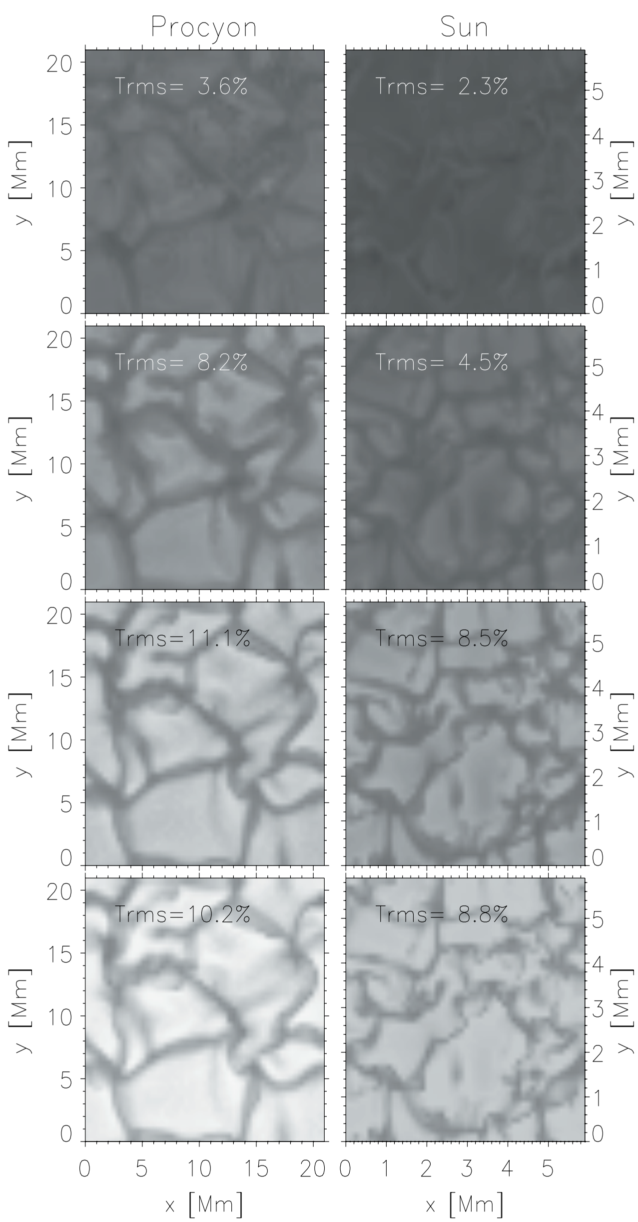

τ = 0.3

τ = 1.0

τ = 3.0

τ = 10

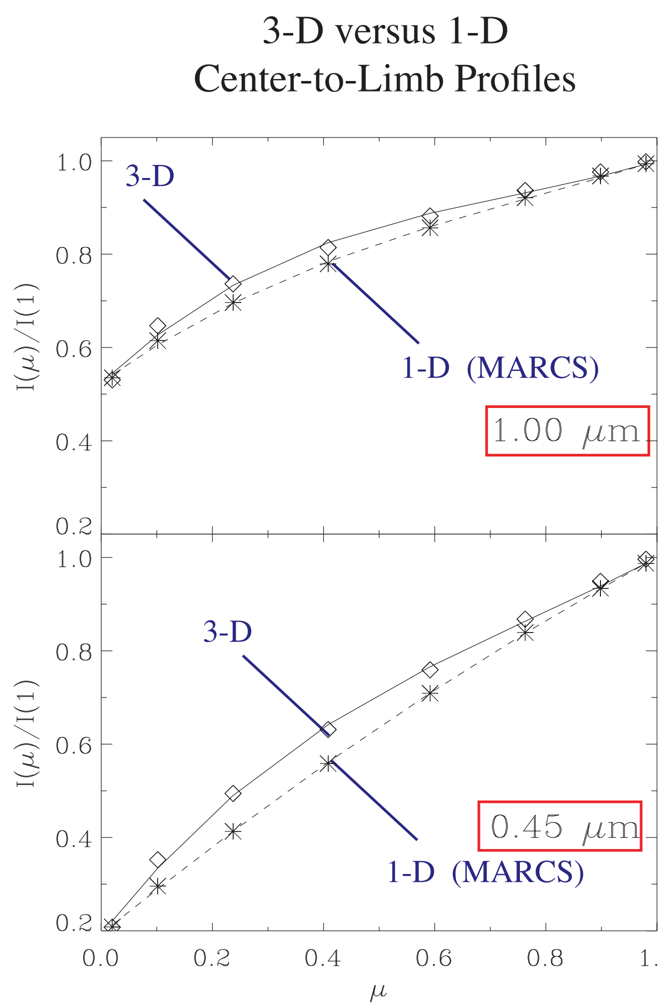

FIG. 19.—Limb darkening for the three-dimensional (*rhombi*) and one-dimensional (*asterisks*) models. Third-order polynomials have been fitted by regular least-squares fits to the data.

Prediction:
1.6 %
angular size
difference
between
1 micron
and
450 nm

A Tail of Three Atmosphere Codes

1) 1-D PHOENIX: A general-purpose state-of-the-art stellar and planetary atmosphere code

Peter Hauschildt

France Allard

Eddie Baron

+ 17 other PHOENIX developers

1-D Spherical Symmetry,
non-LTE line blanketing,
MLT convection,
Expanding Atmospheres

See: Hauschildt & Baron (1999) J. Comp. and App. Math, 109, 41
and
Aufdenberg et al. (2002) ApJ 570, 344

2) 3-D CO^{5}BOLD: The ``COservative COde for COmputation of COmpressible COnvection in a BOx of L Dimensions"

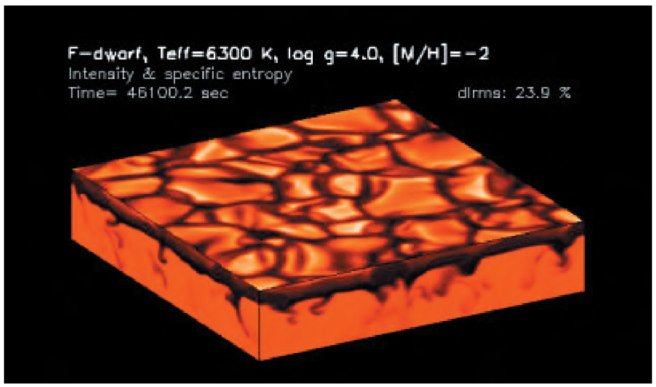

Hans-Günther Ludwig

3-D hydrodynamics,
plane parallel
non-grey opacities

See: Freytag, Steffan & Dorch (2002) Astronomische Nachrichten, 323, 213.

3) 1-D ATLAS 12: Latest version of the Kurucz atmosphere and spectrum synthesis code

1-D Plane-Parallel
LTE line-blanketing
MLT convection with "Overshooting Approximation"

See: http://kurucz.harvard.edu/
and
Castelli, Gratton & Kurucz (1997) A&A 318, 841

A CO^{5}BOLD model for Procyon

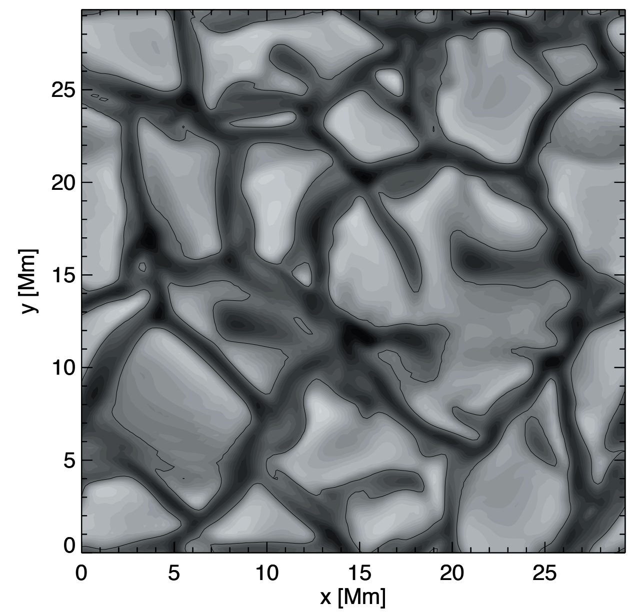

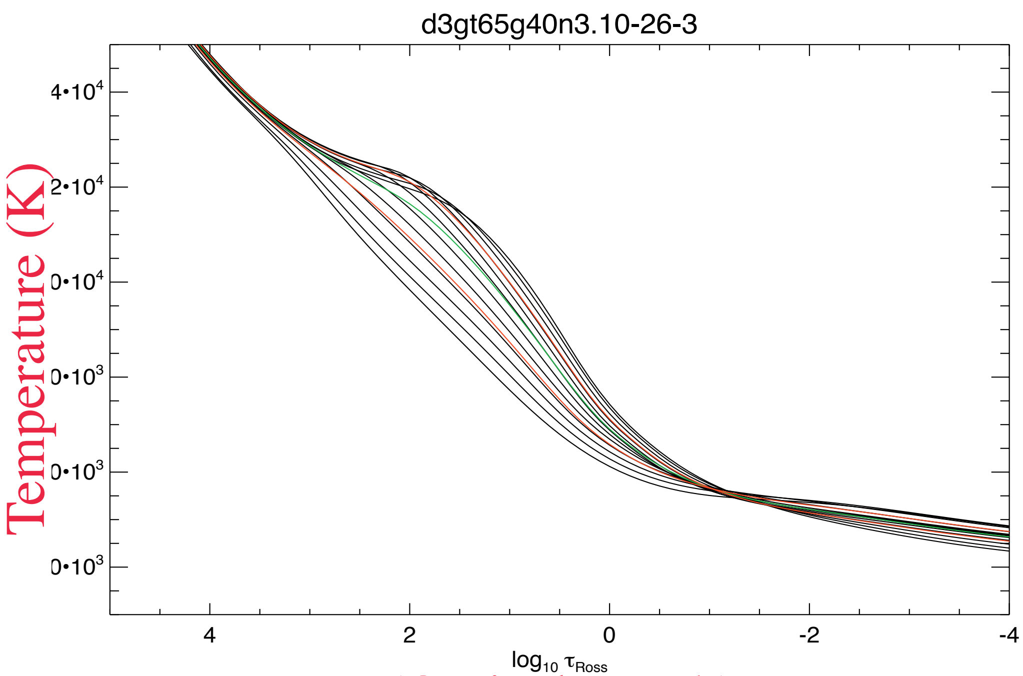

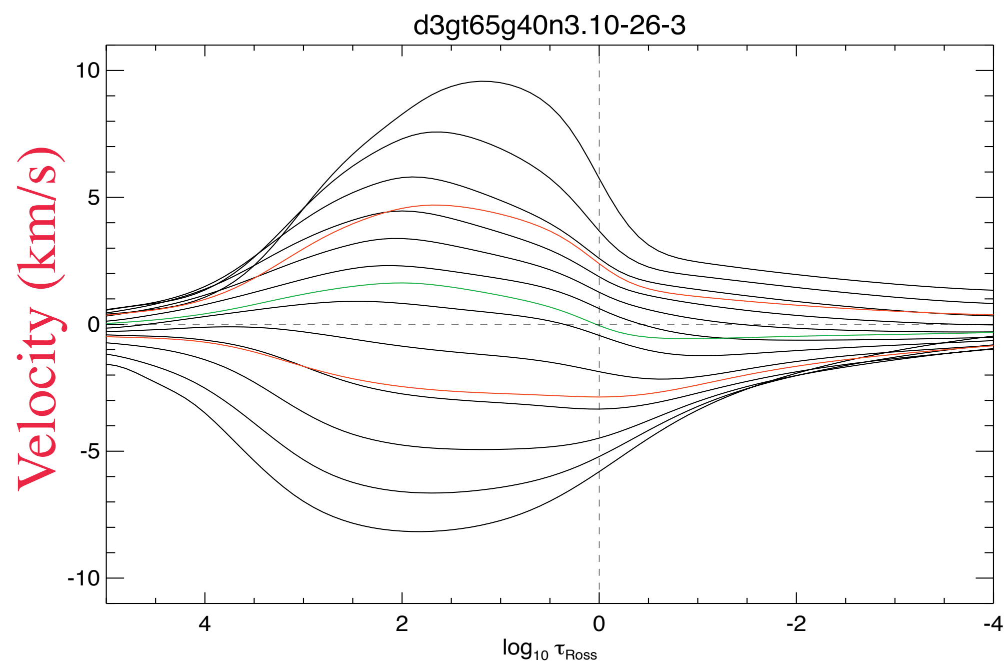

Model intensities → Model visibilities

The **visibility** V is the Hankel transform of a set of **intensities** I, **angles** μ, and **angular diameter** θ_{LD}

$$V(B,\lambda) = \int_0^1 S(\lambda) I(\mu,\lambda) \left[\pi\theta_{LD}(B/\lambda)(1-\mu^2)^{1/2}\right] \mu \, d\mu$$

Squared visibility for a **baseline** B and **mean wavelength** λ_0 for **filter transmission** $S(\lambda)$:

$$V(B,\lambda_0)^2 = \frac{\int_0^\infty V(B,\lambda)^2 \, d\lambda}{\int_0^\infty S(\lambda)^2 \; F(\lambda)^2 \quad d\lambda}$$

$$\lambda_0 = \frac{\int_0^\infty \lambda \, S(\lambda) \; F(\lambda) \; d\lambda}{\int_0^\infty S(\lambda) \; F(\lambda) \; d\lambda}$$

Flux: $F_\lambda = \int_0^1 I(\mu,\lambda) \; \mu \; d\mu$

Mark III and VLTI: Optical and Near-IR Interferometry

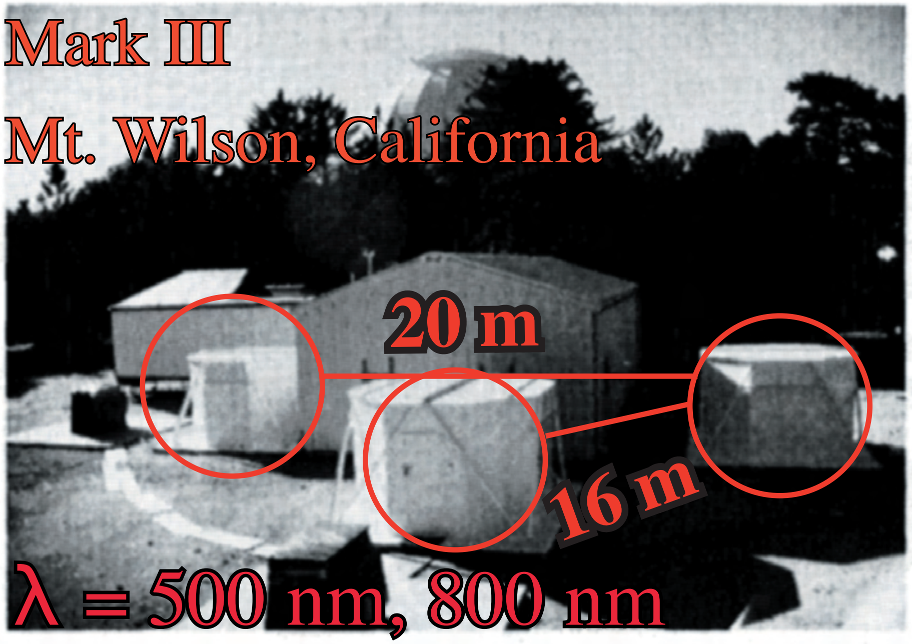

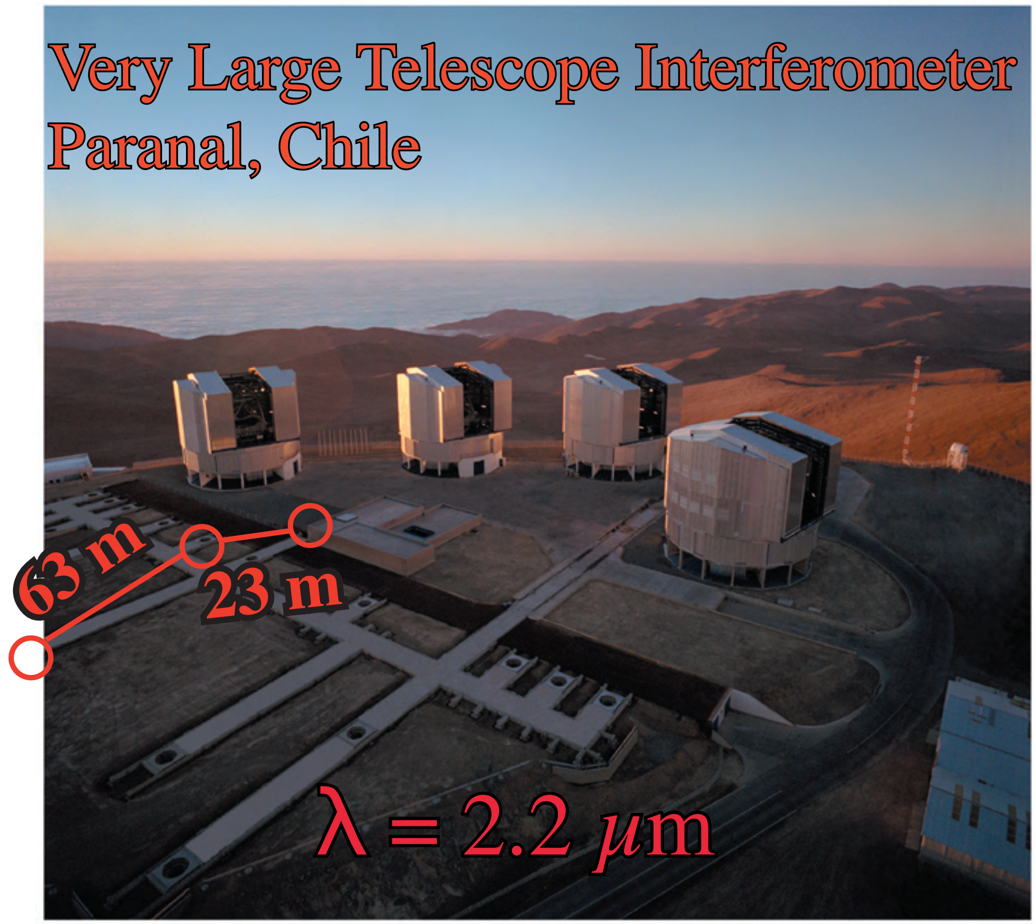

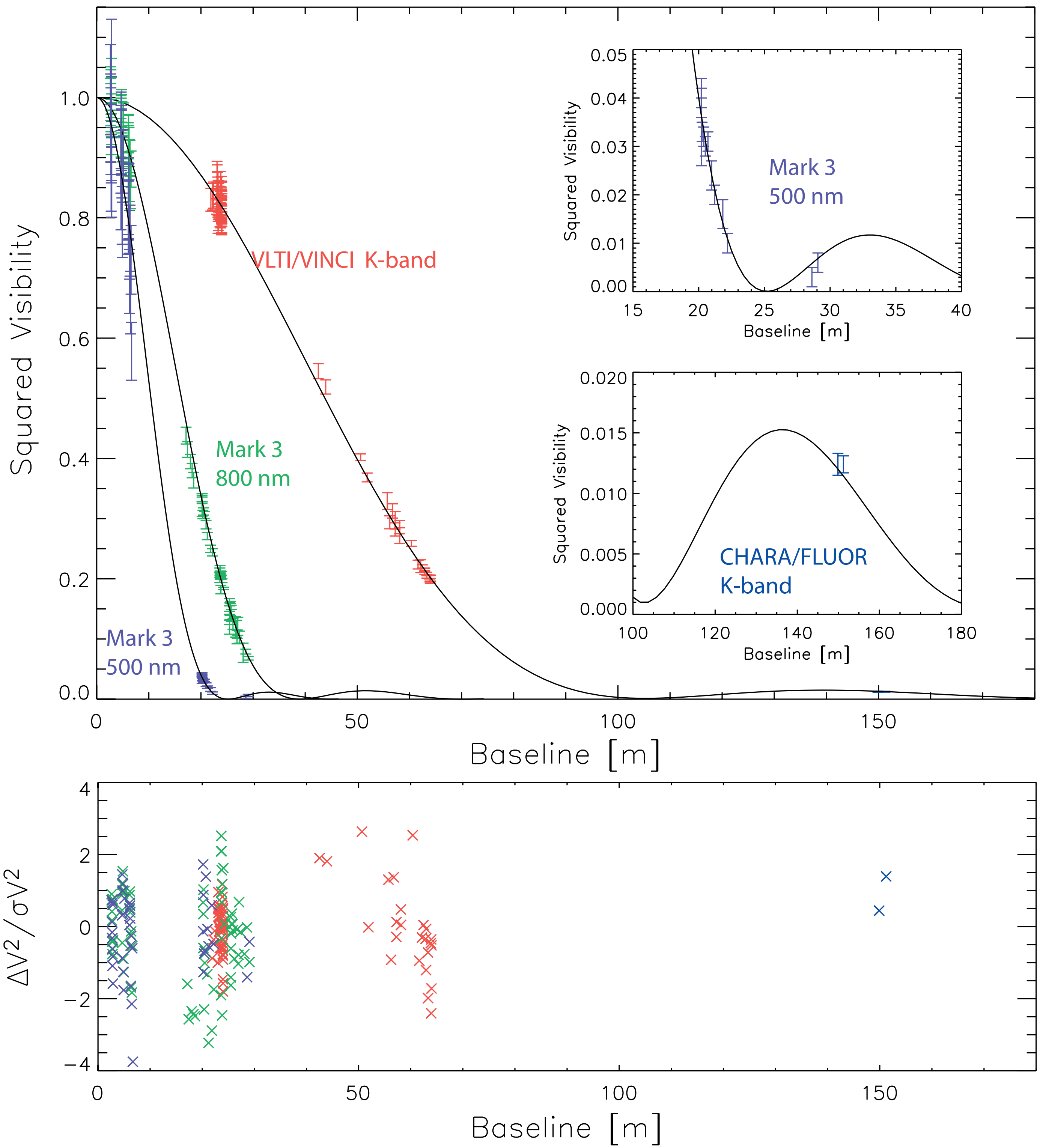

3-D CO^{5}BOLD Model 5.392 mas

vs.

Mark III 500 nm, 800nm VLTI/VINCI K-band and CHARA/FLUOR K-band

Angular Diameters from 1-D & 3-D Model Fits

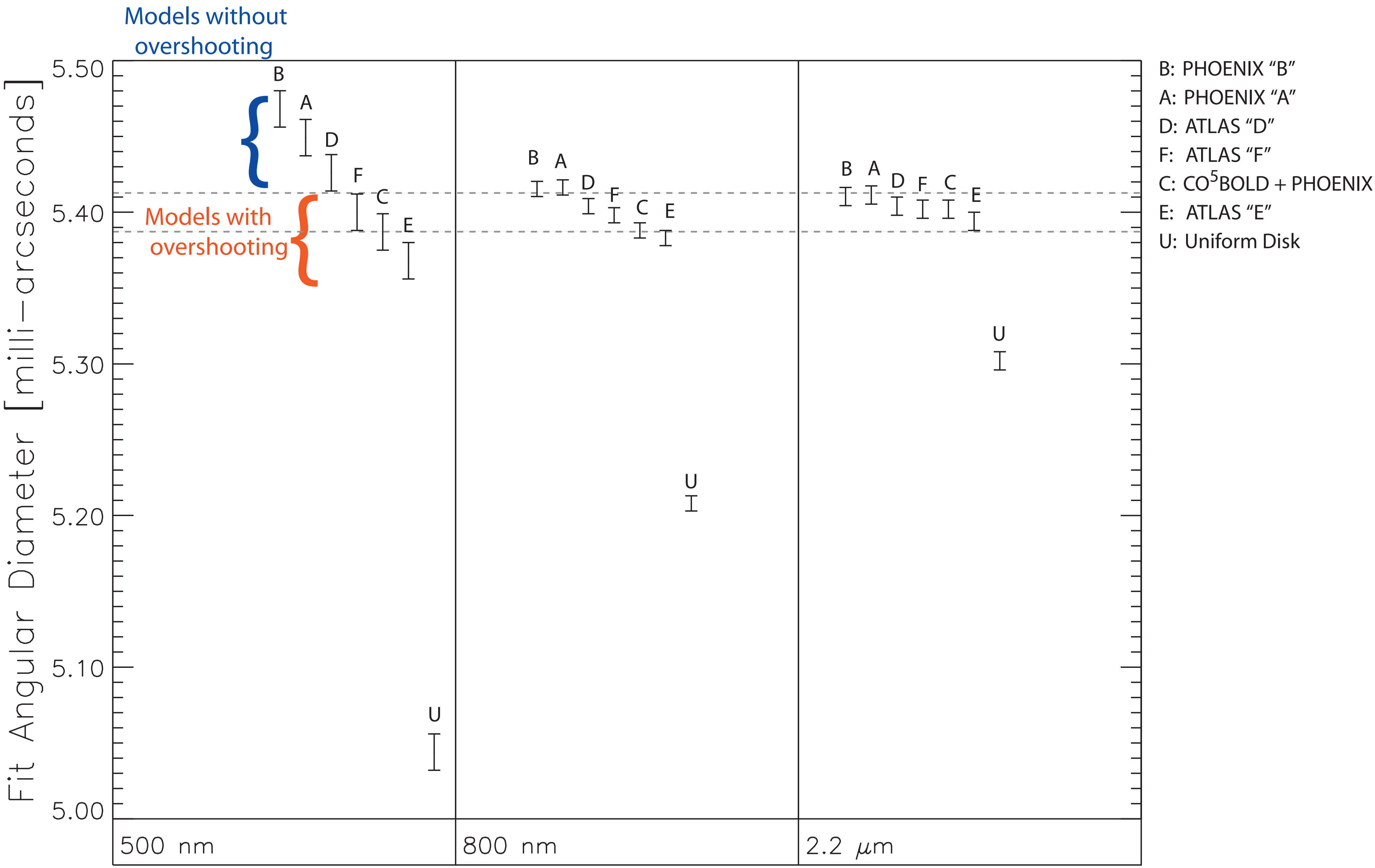

Comparing 1-D and 3-D Model Temperature Structures

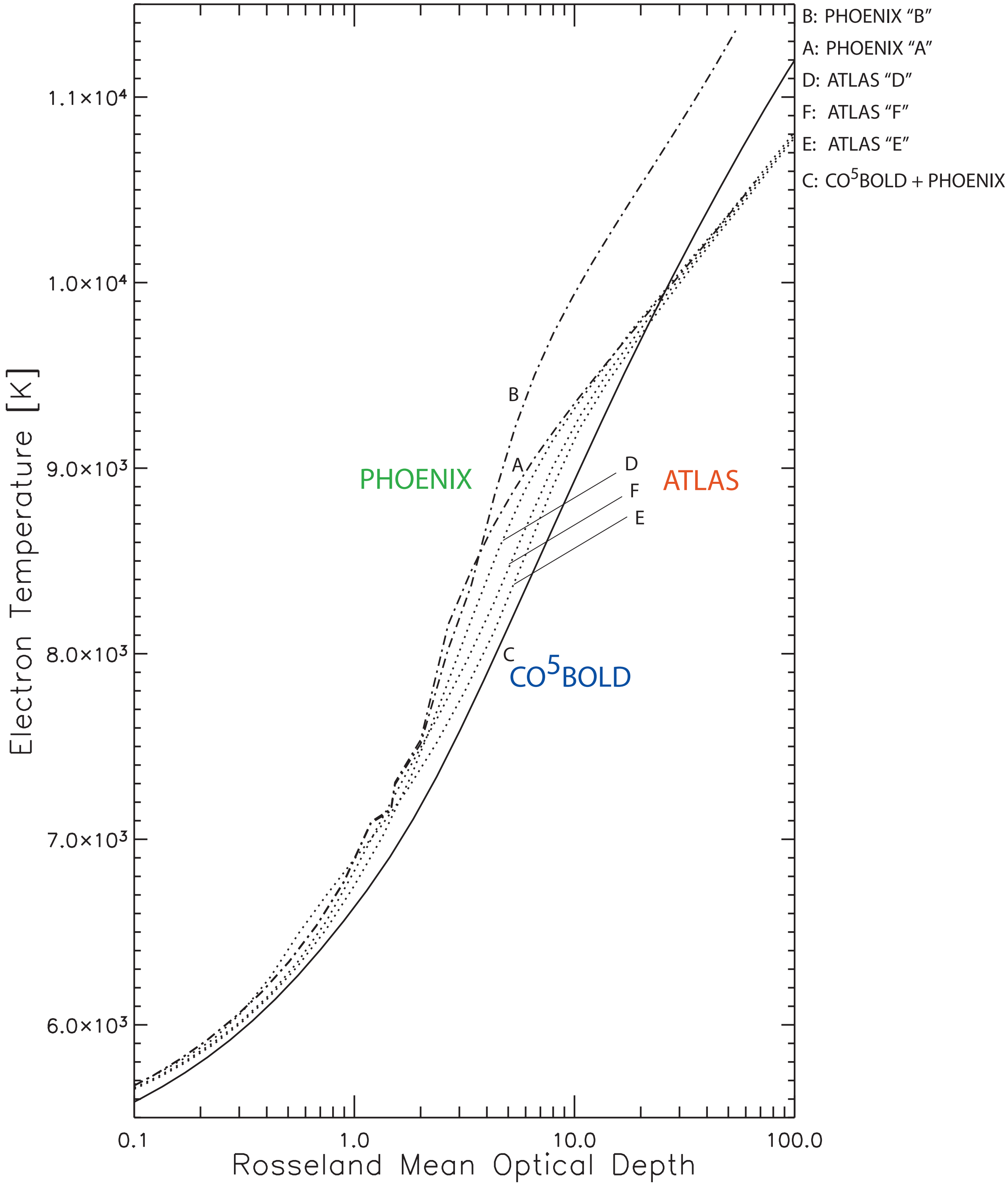

Procyon's 2-D Surface: Many Temperatures, Many Colors

Model Intensity Map

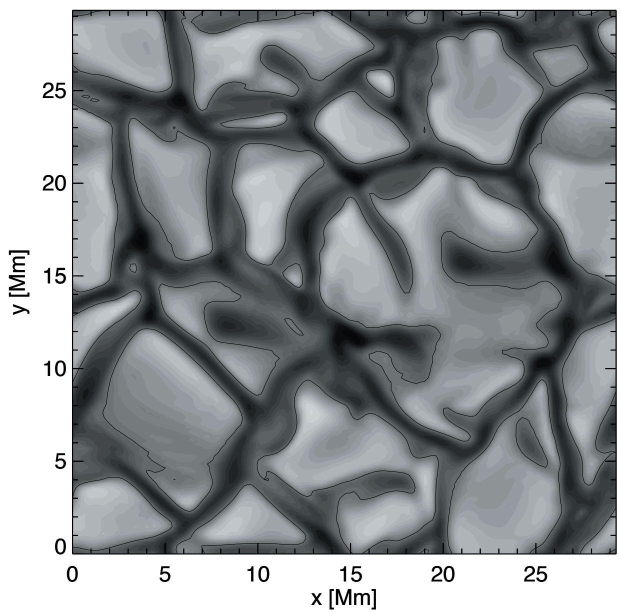

Intensity Historgram

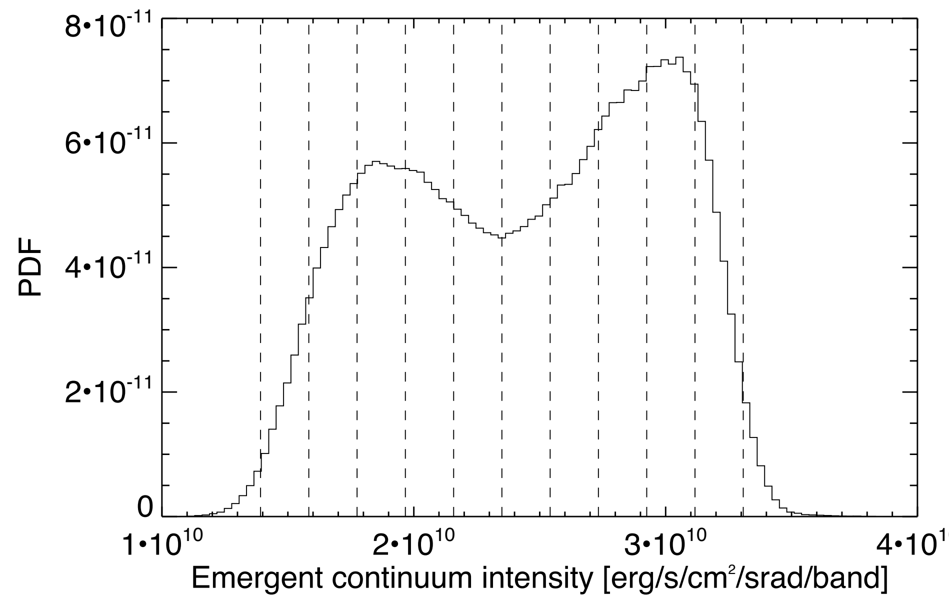

Procyon's Spectral Energy Distribution vs. Composite Model Spectrum

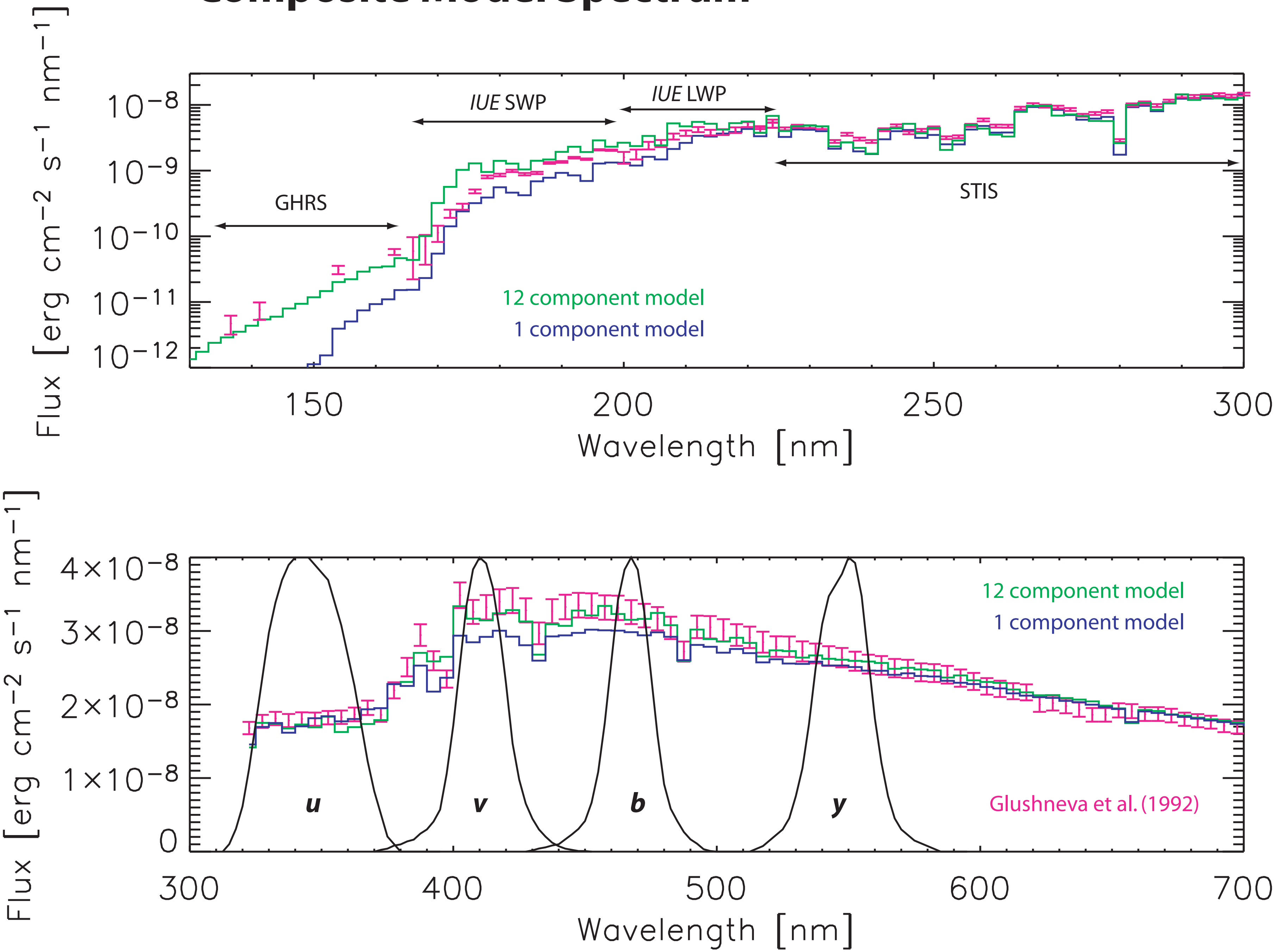

Synthetic vs. Observed Strömgren Photometry

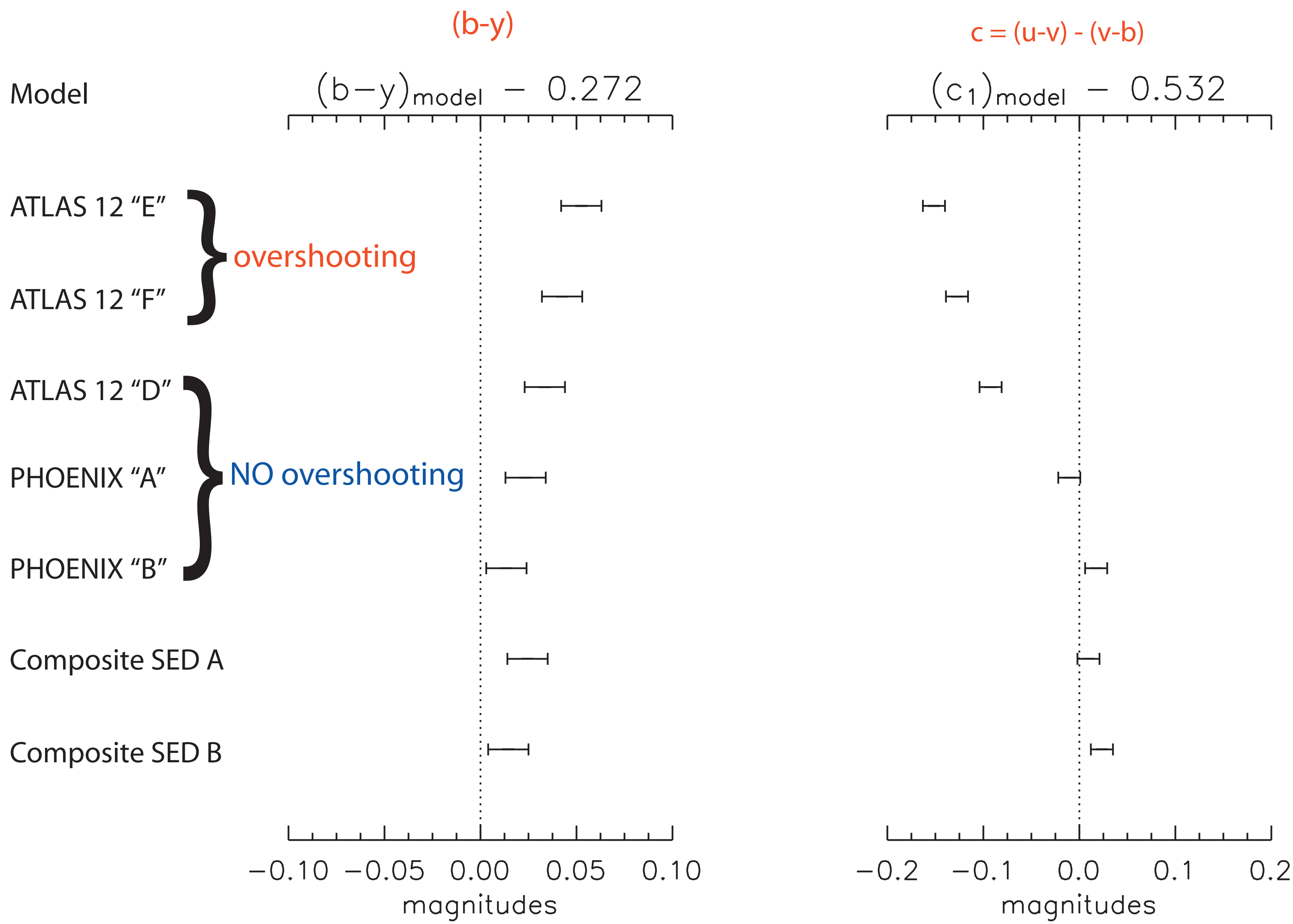

Part II

Deneb & Rigel, Stellar Winds, and Limb Darkening

From F5 IV to A2 Ia & B8 Ia...

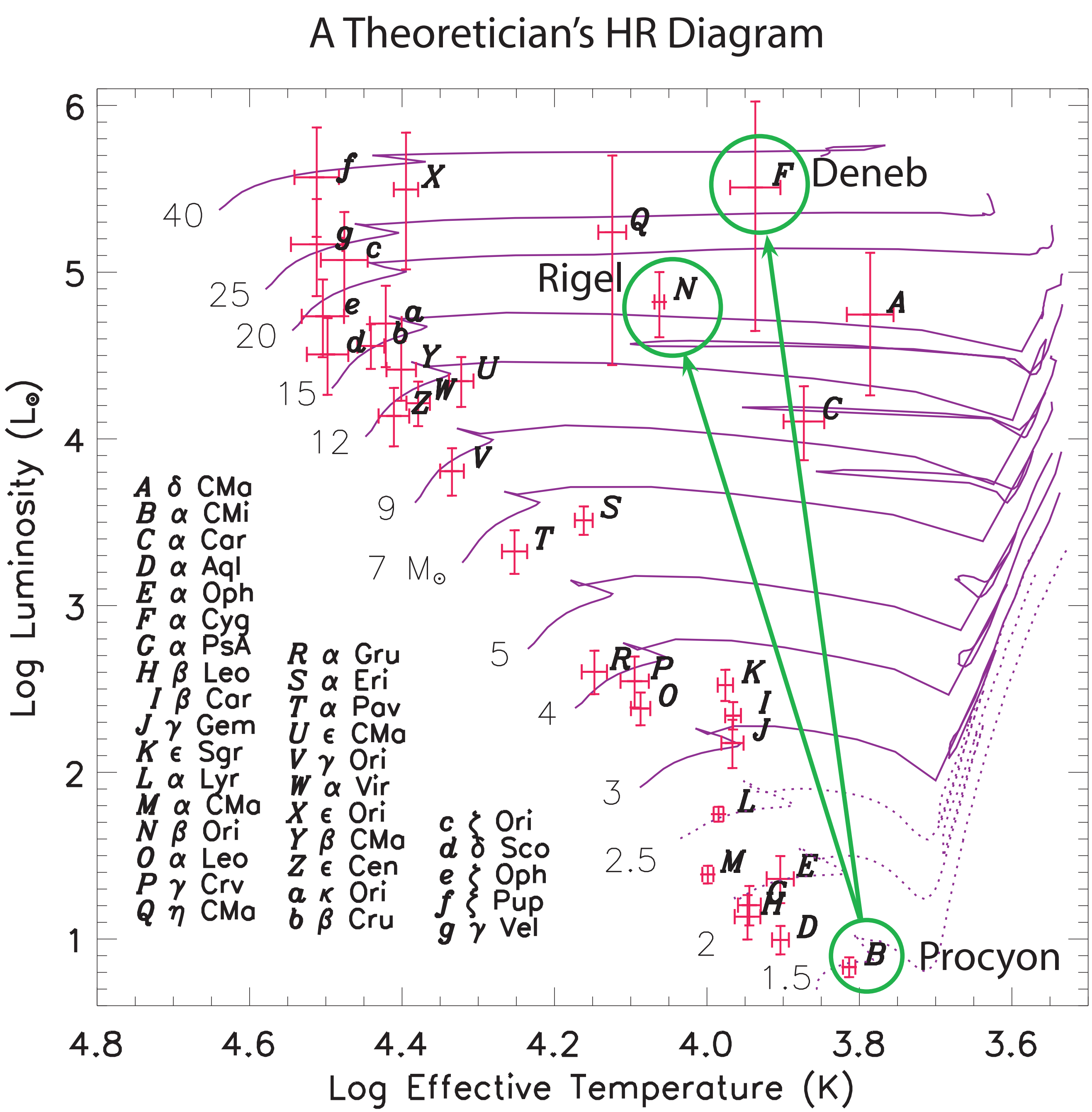

Angular Diameters from Hanbury Brown *et al.* (1974) Aufdenberg *et al.* (2002)

Distances from HIPPARCOS

Tracks from Schaller *et al.* (1992) and Girardi *et al.* (2000)

Plane Parallel vs. Spherical Limb Profiles

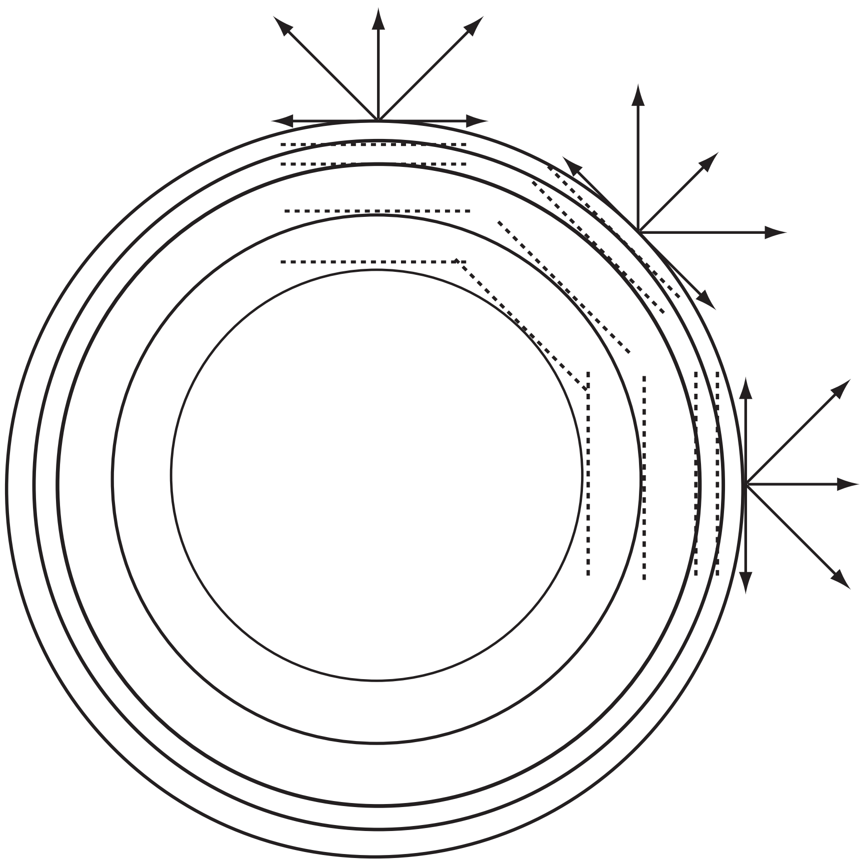

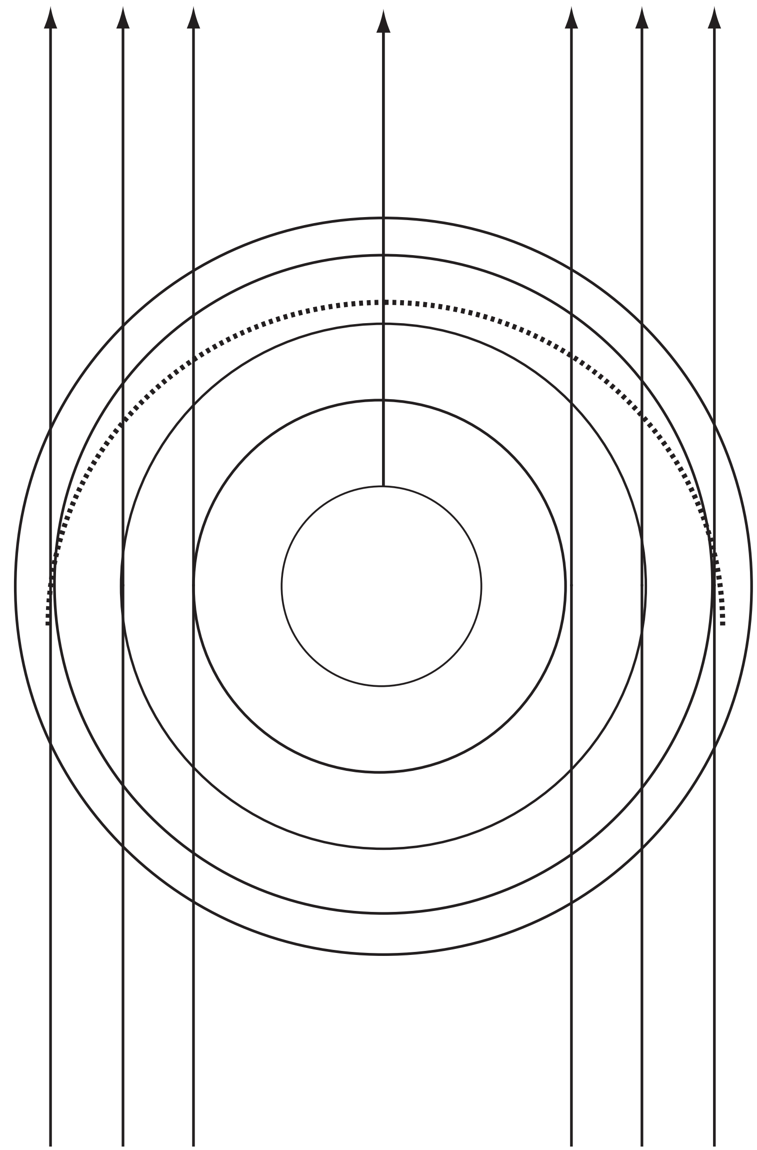

Plane Parallel Limb Profiles

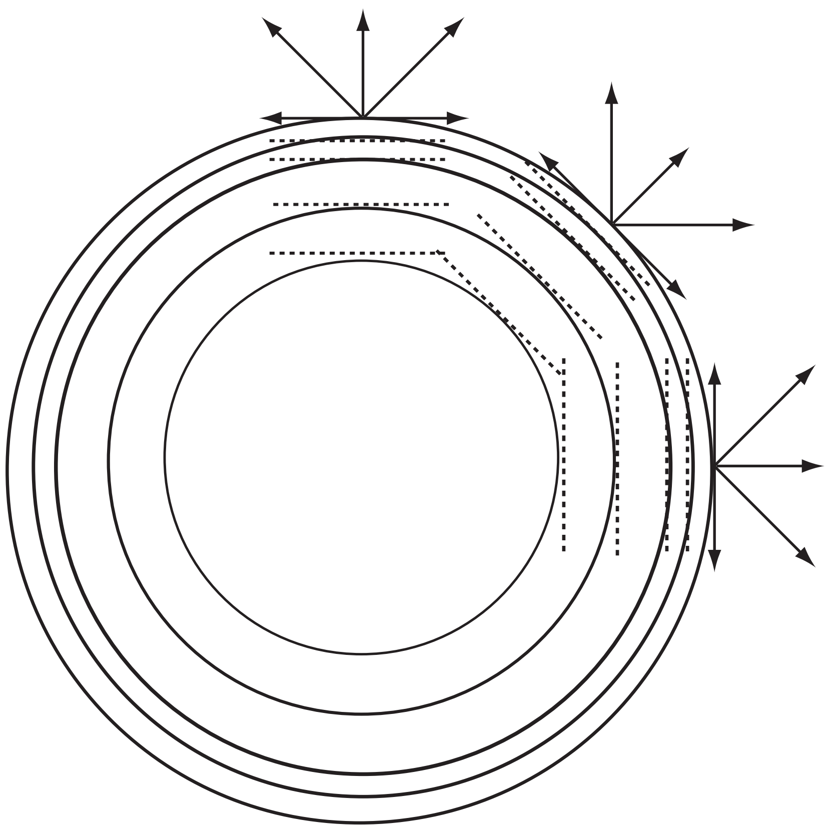

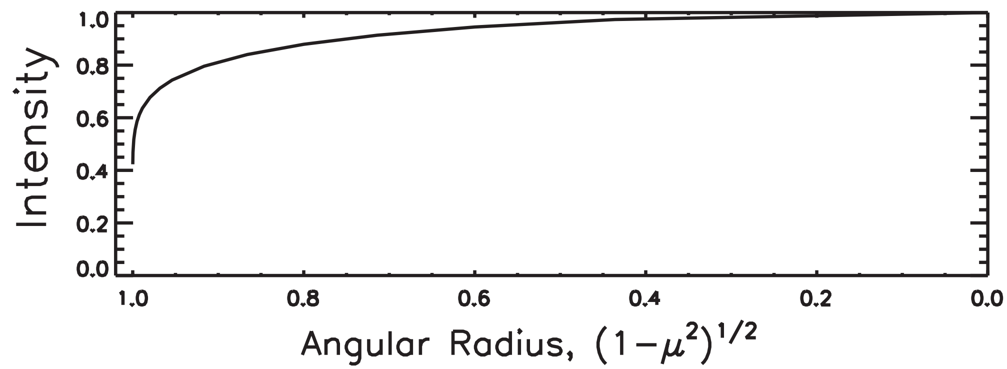

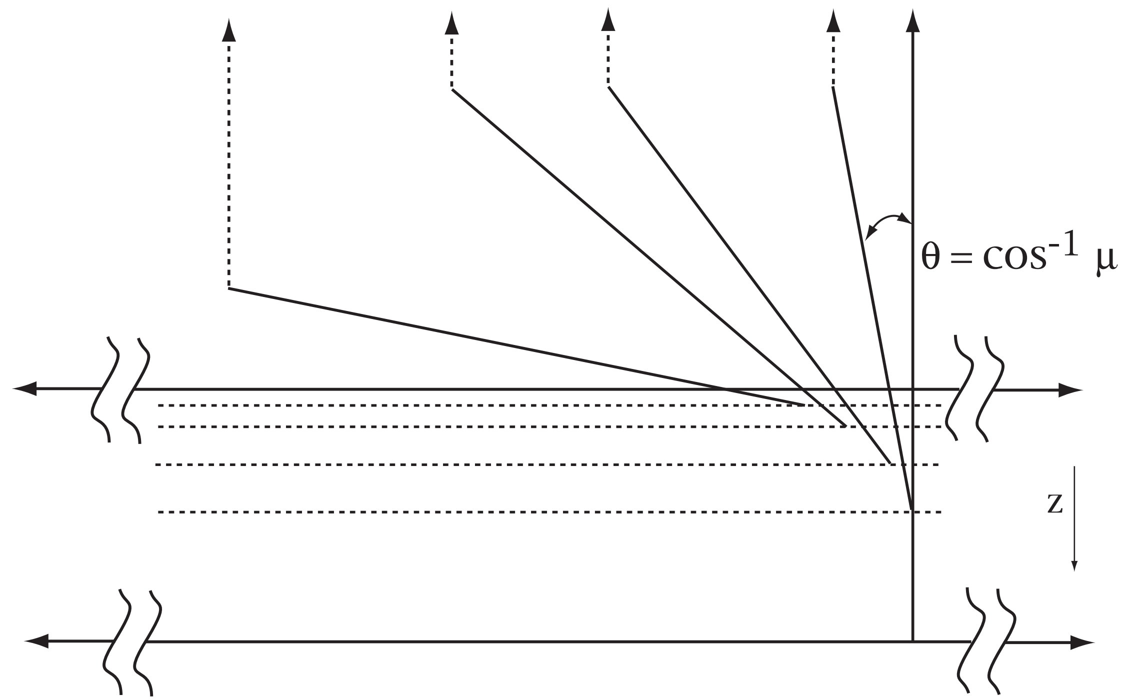

Spherical Limb Profiles

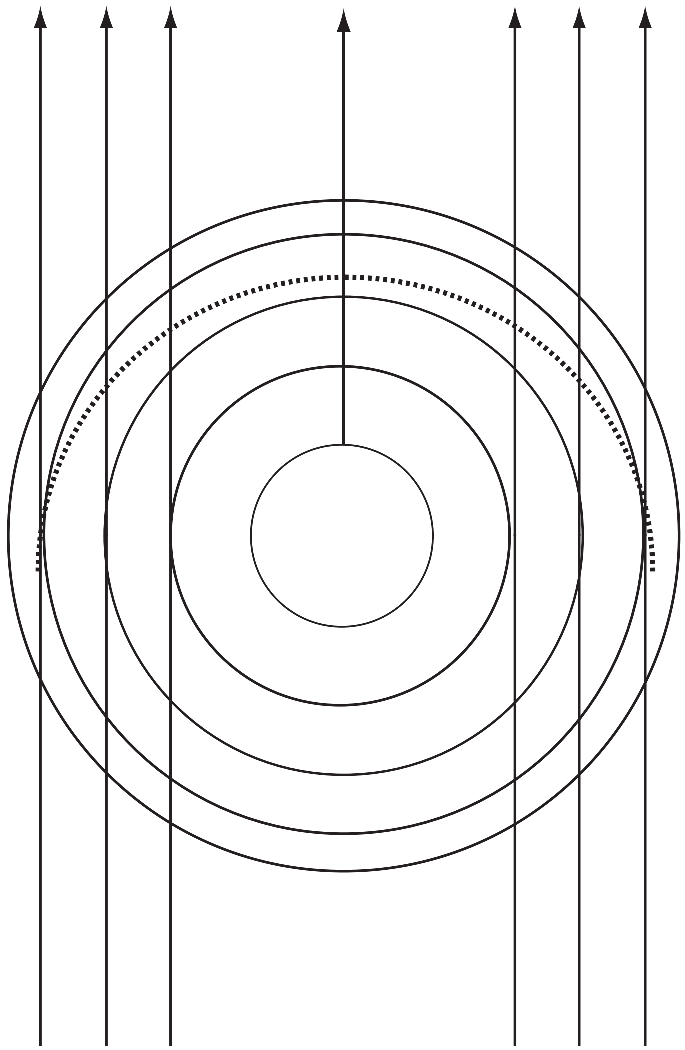

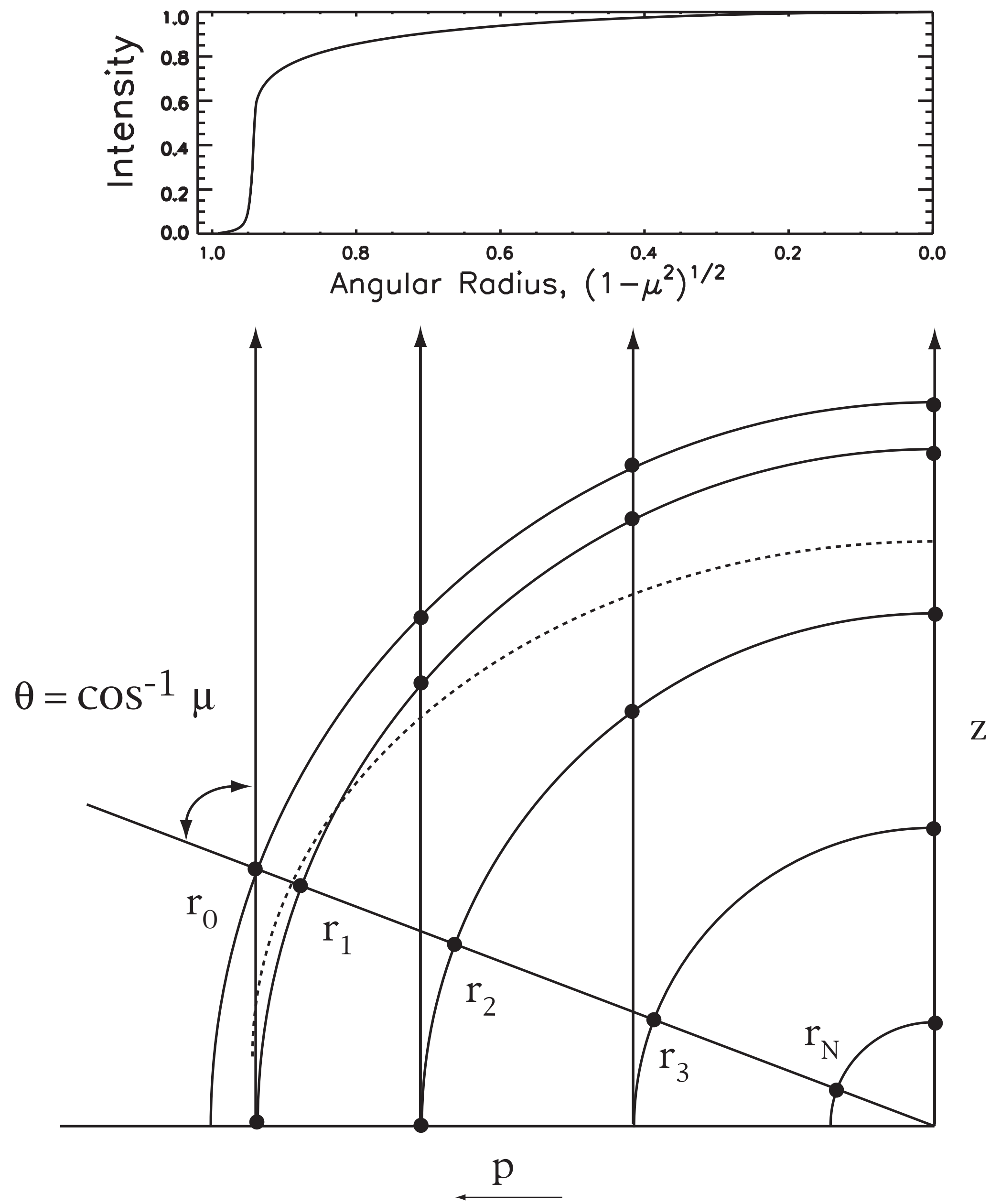

Deneb (α Cygni): the prototypical A-type supergiant

The wind momentum-luminosity relationship of galactic A- and B-supergiants

R.P. Kudritzki[1,2,3], J. Puls[1], D.J. Lennon[1,4], K.A. Venn[5], J. Reetz[1], F. Najarro[9], J.K. McCarthy[6], and A. Herrero[7,8]

mass-loss rate, velocity, luminosity, radius

$$\dot{M}\, v_\infty \propto L_*^{1/\alpha} / R_*^{1/2}$$

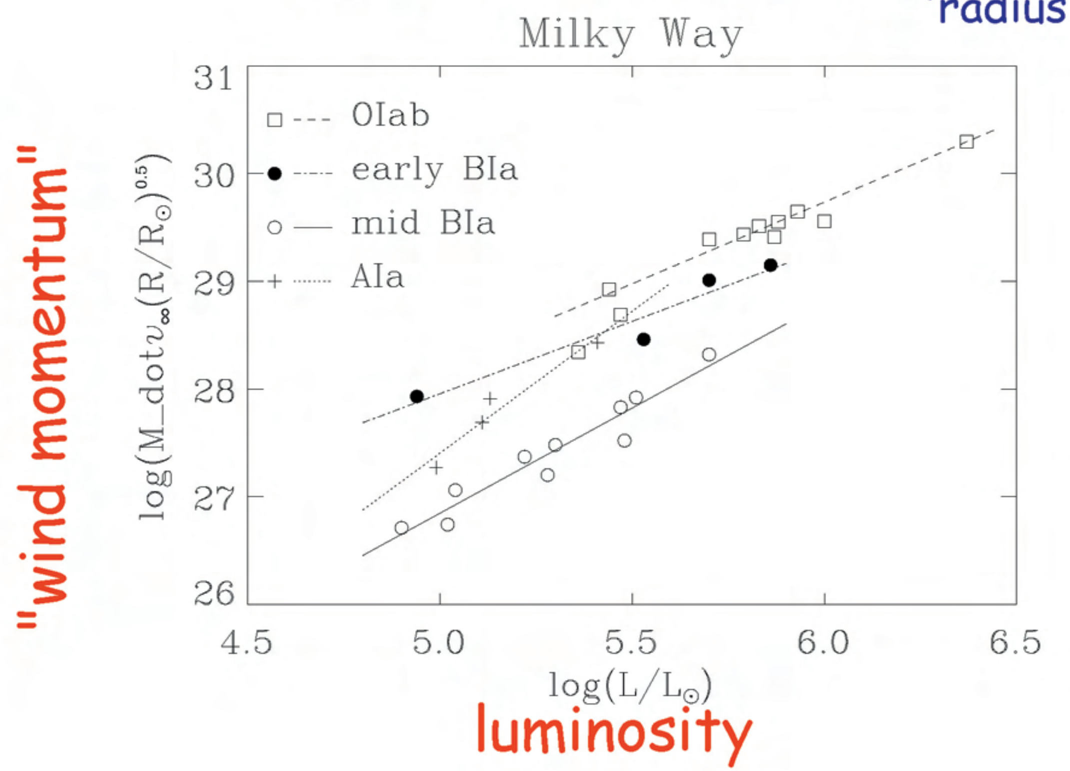

Mass Loss Rate Diagnostics

* P-Cygni Line Profiles

* Bremsstrahlung Excess IR - mm -Radio

* Stellar Limb Profile

New!

Deneb's Stellar Wind: Ultraviolet to Radio Constraints

Mg II h&k double P-Cygni lines

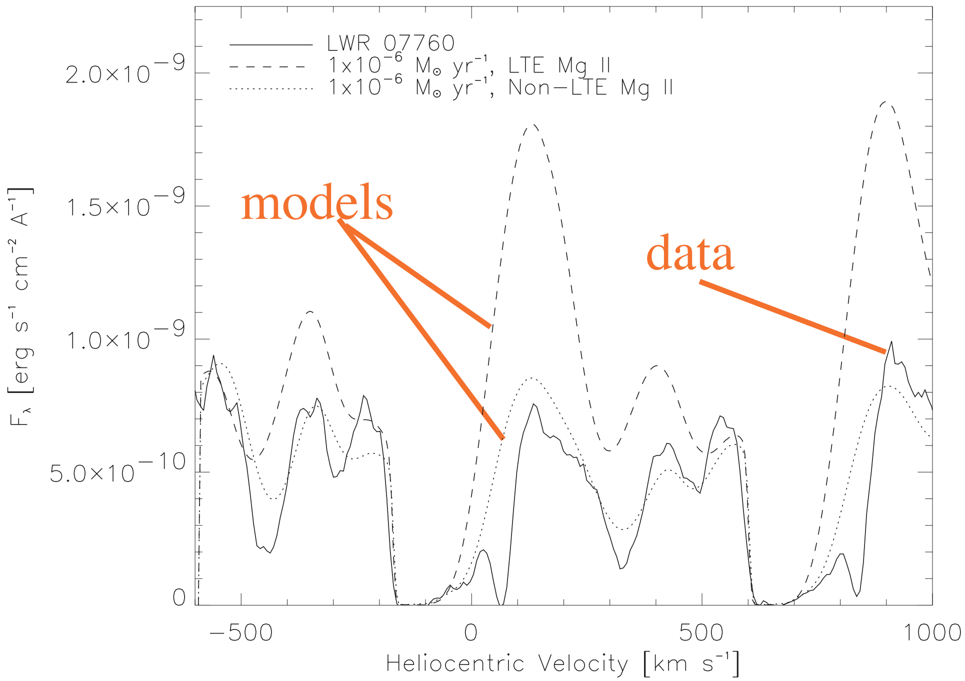

IR, mm, radio continuum

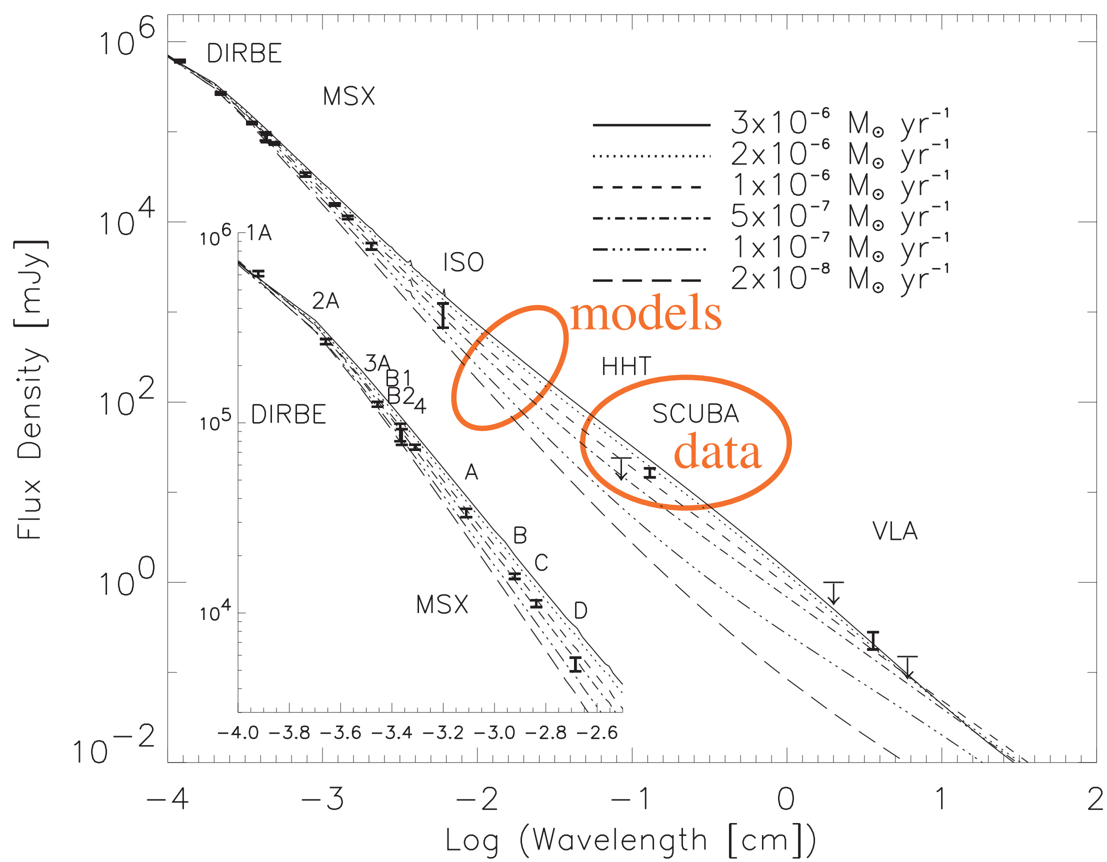

Aufdenberg et al. (2002) ApJ 570, 344

NPOI and CHARA: *More* Optical and Near-IR Interferometry

Navy Prototype Optical Interferometer
Flagstaff, Arizona

$\lambda = 650 - 850$ nm

Center for High Angular Resolution Astronomy Array
Mt. Wilson, California

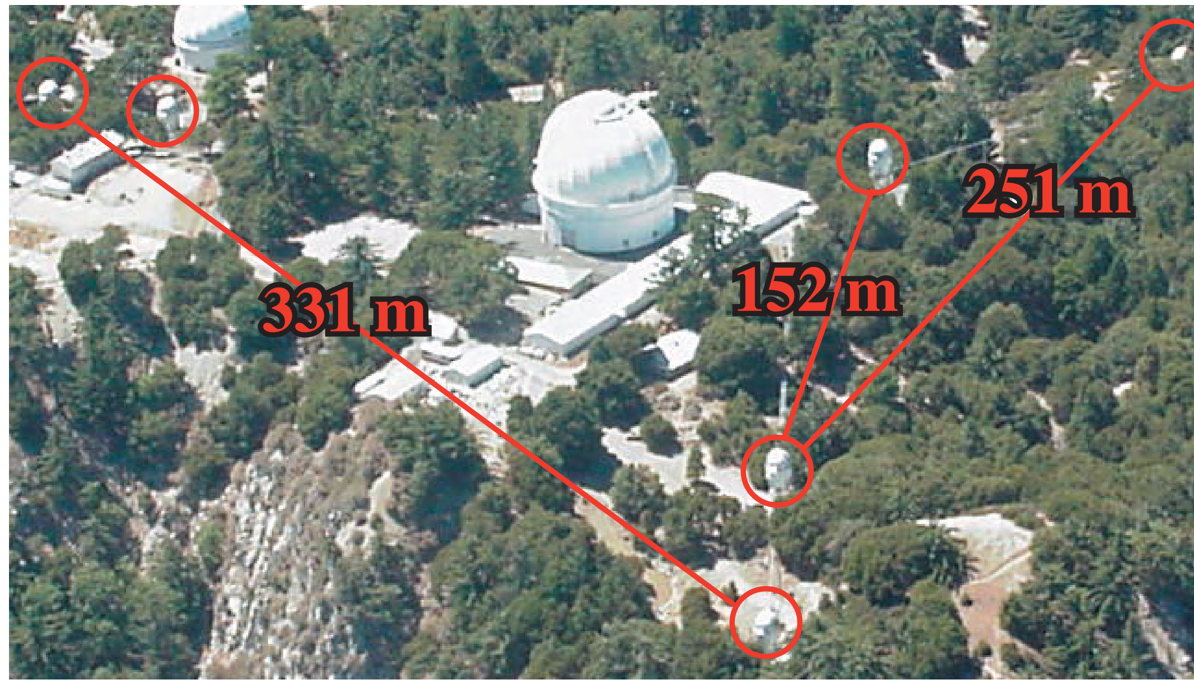

$\lambda = 2.2\ \mu m$

Deneb: NPOI 1st lobe data and 2nd lobe model predictions

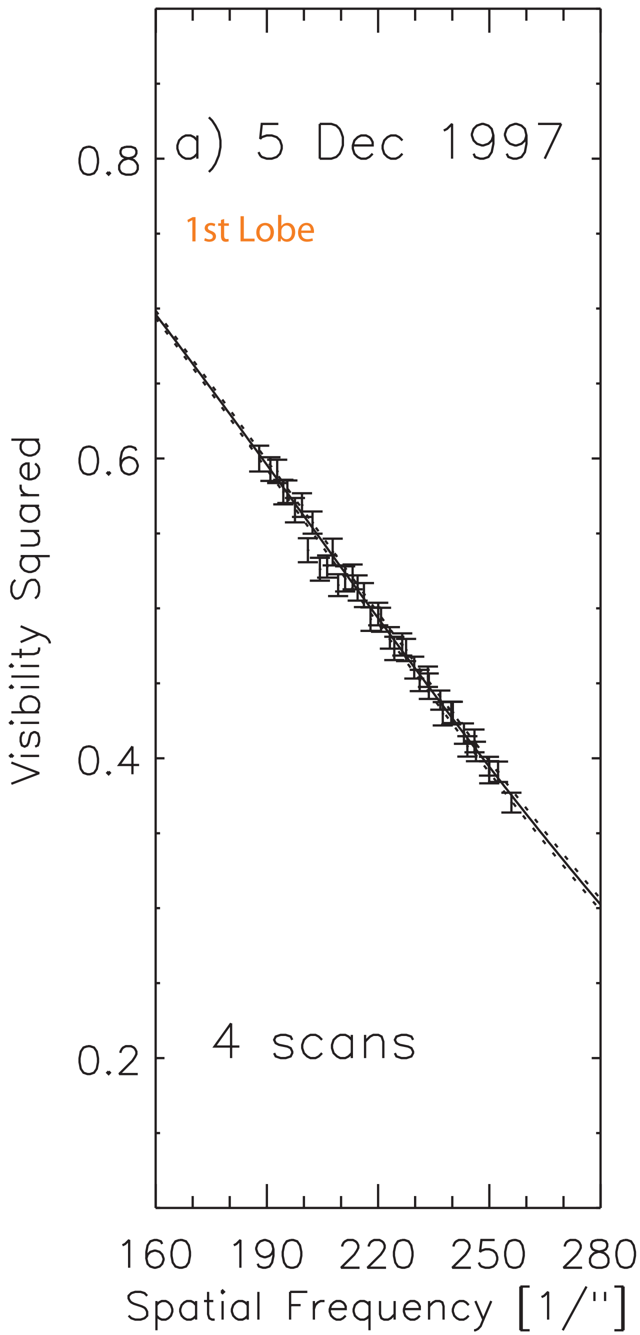

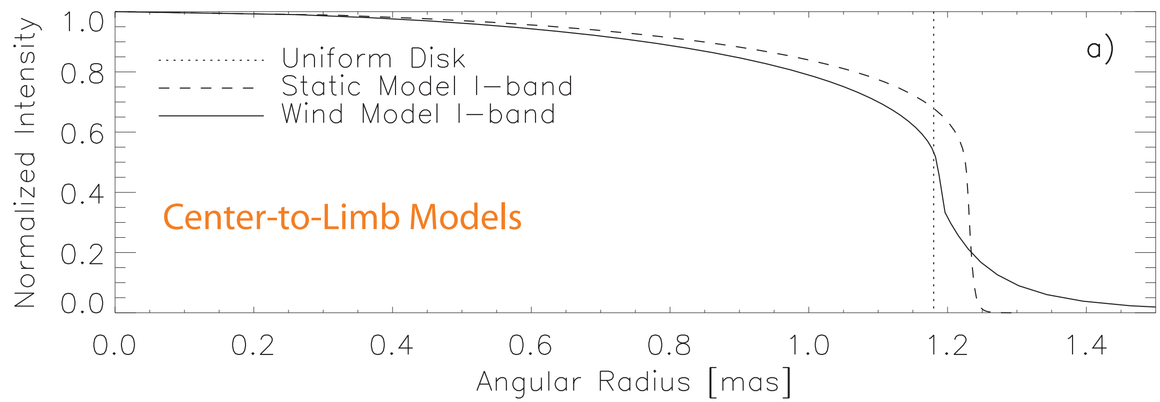

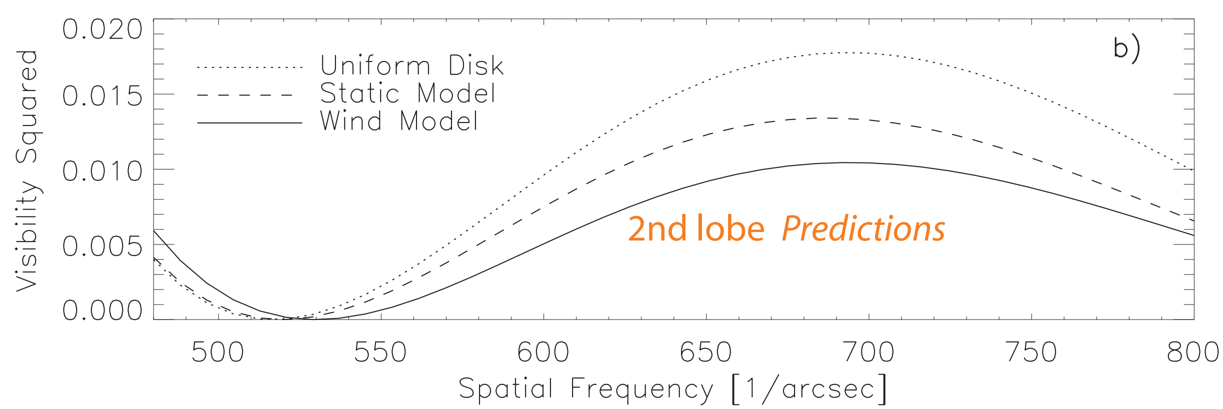

Aufdenberg *et al.* (2002) ApJ 570, 344

2004 CHARA/FLUOR Observations of Deneb: Wind Detected!

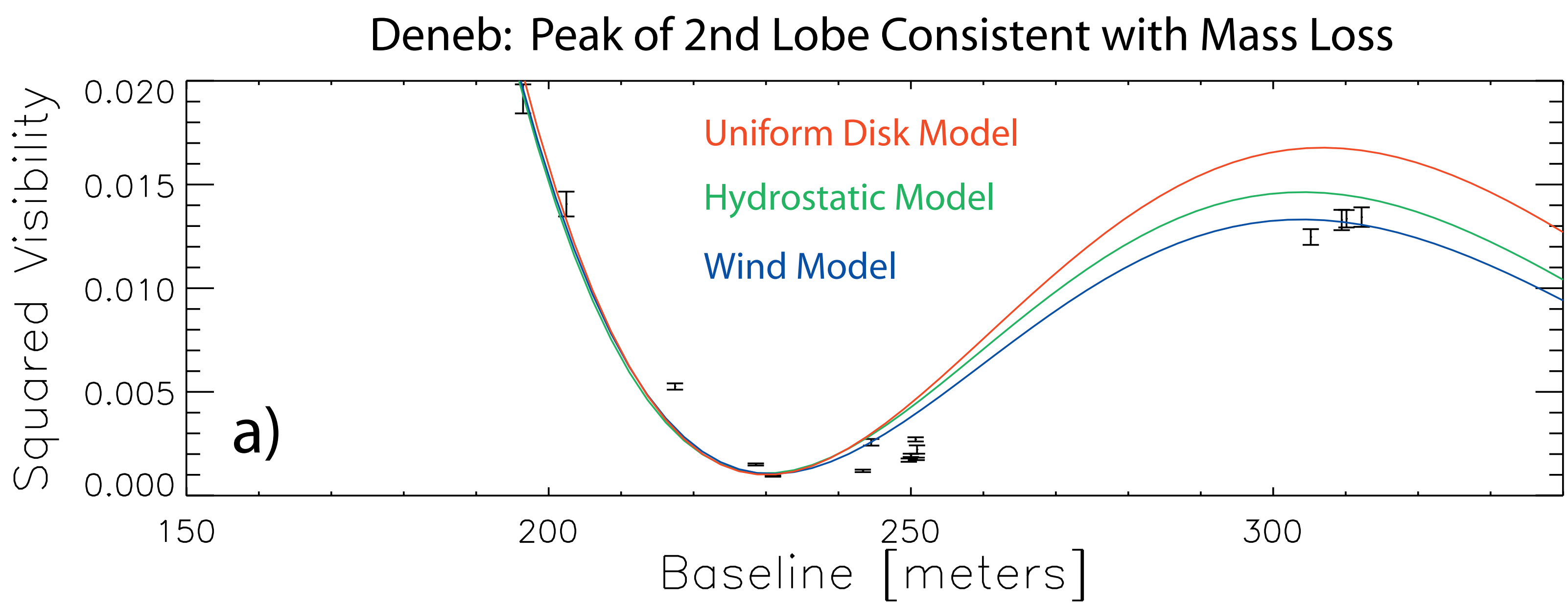

A Surprise! Deneb Appears Asymmetric

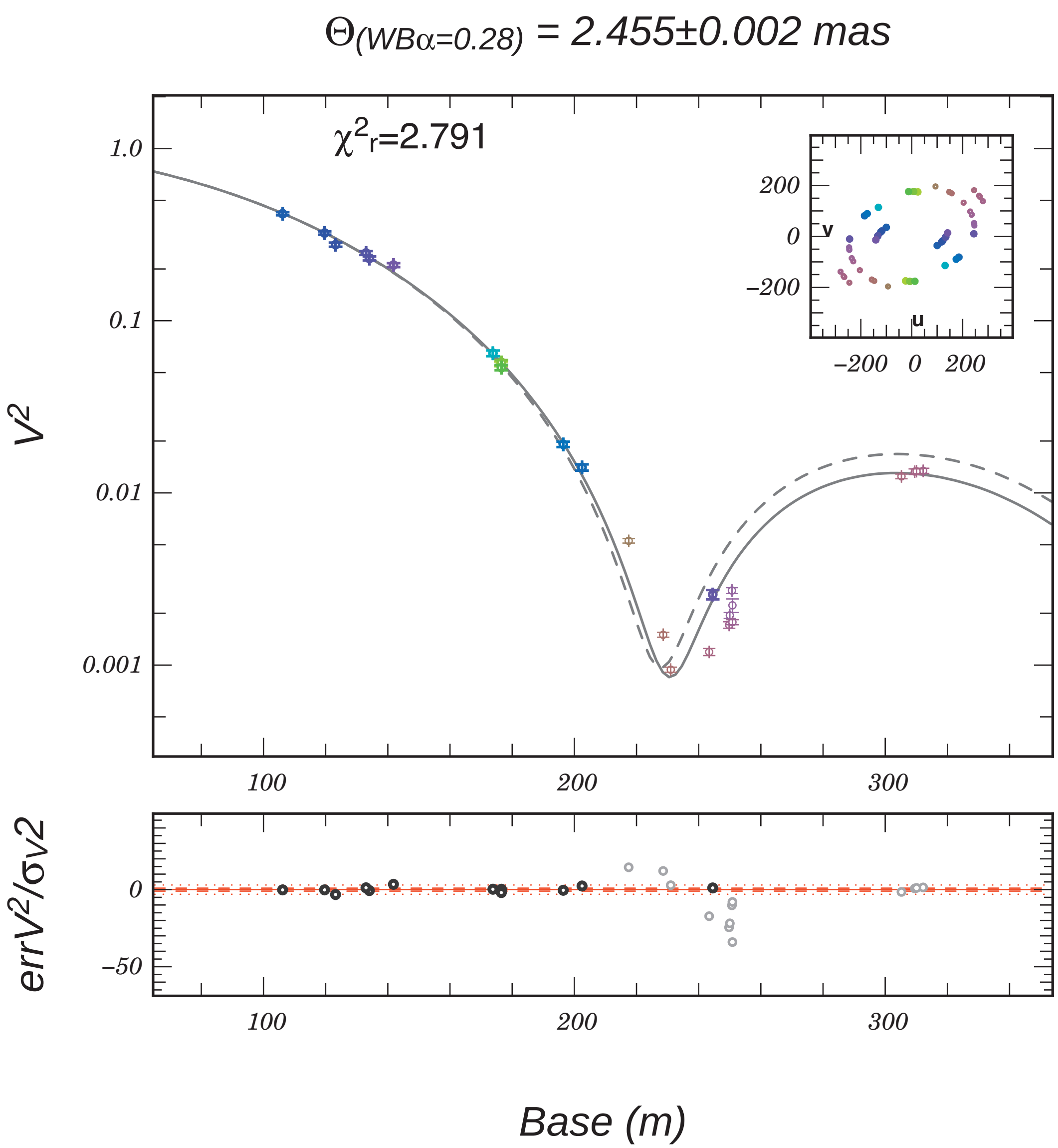

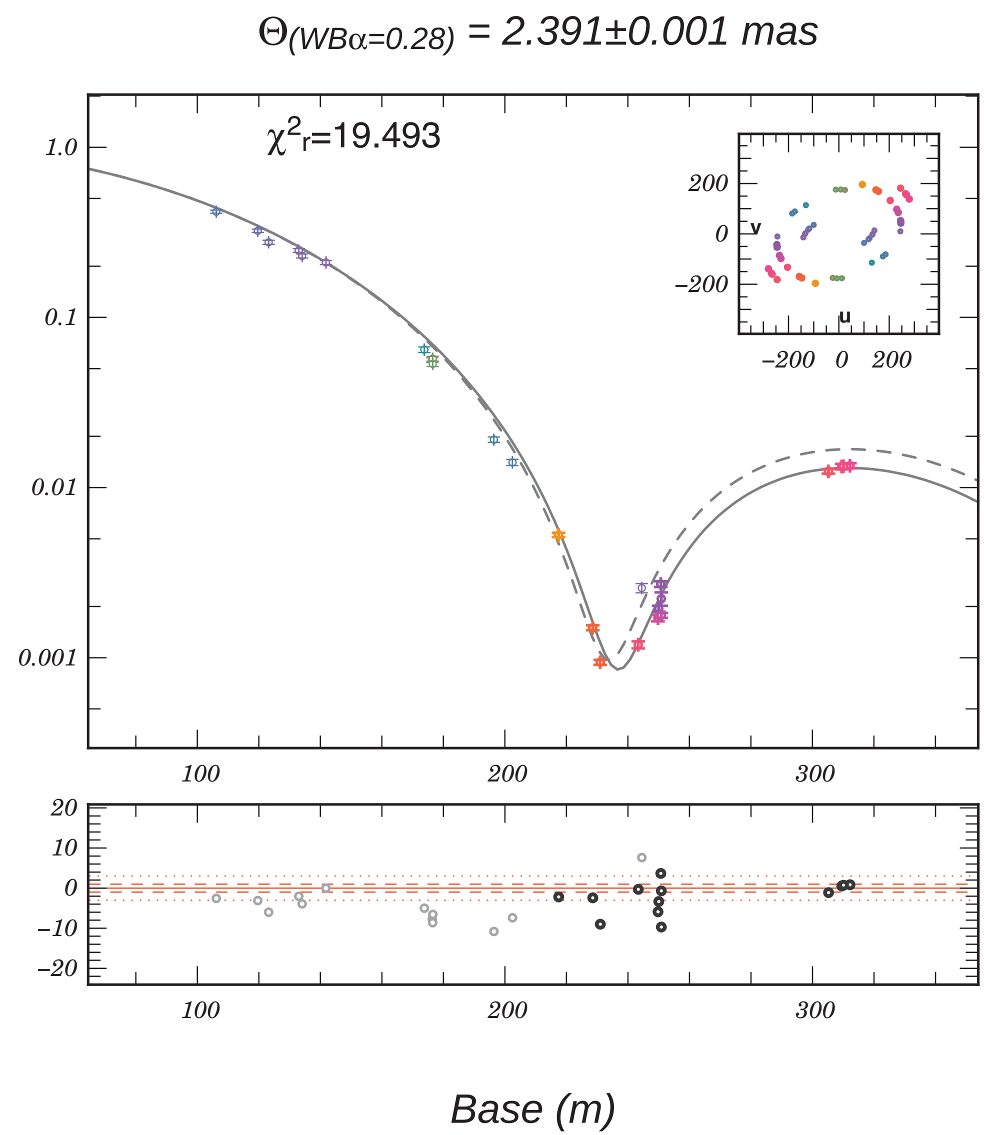

Rigel = β Orionis

Fundamental Parameters constrained by observations

$F_{bol} = (38.6 \pm 2.0) \times 10^{-9}$ W m^{-2}
$\theta_{Ross} = 2.75 \pm 0.01$ mas
$T_{eff} = 11117 \pm 140$ K
$R = 70 \pm 13\ R_\odot$
$\mathrm{Log}(L/L_\odot) = 4.8 \pm 0.2$

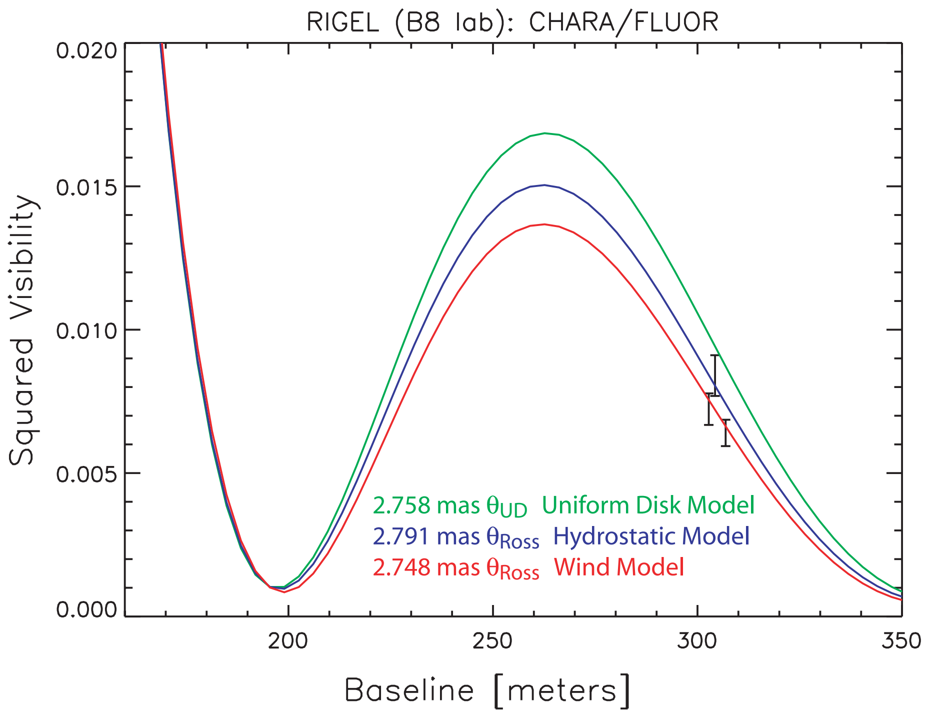

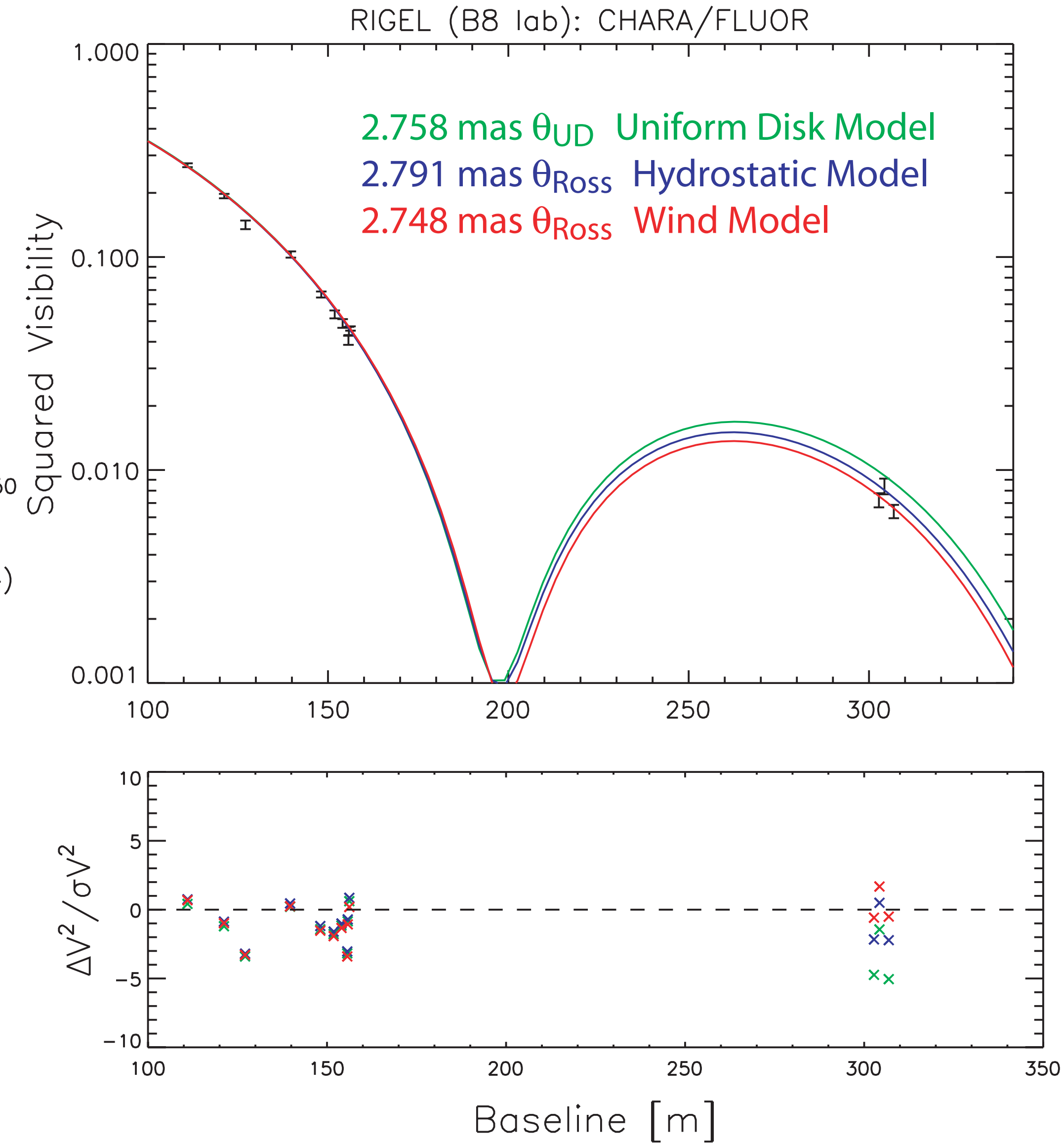

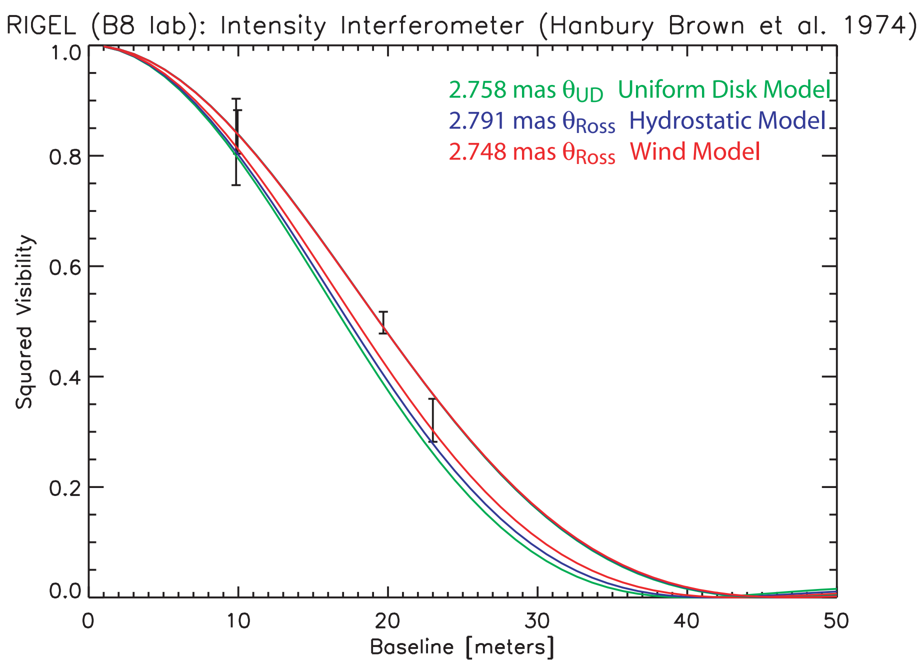

Summary

1. Multi-wavelength (optical + near-IR) visibility measurements are providing very-high precision angular diameters: ≈ 0.1%. Such measurements can tightly constrain limb-darkening.

2. For Procyon, such measurements test models with different temperature gradients due to different convection treatments. 3-D predictions are confirmed: Procyon's limb less darkened than most 1-D models predict.

3. 1-D models can be made to fit observed limb darkening, but can't to match full SED. For Procyon, the mean temperature structure appears to be partially decoupled from its mean photometric colors. What do precise colors tell us about T_{eff} and convection?

4. Visibility measurements of Deneb yield a mass-loss rate consistent with UV and radio diagnostics, but uncertainties are still large (>> 15%), but now within an order of magnitude.

5. Deneb's stellar disk appears to asymmetric at ~3% level, asymmetric outflow?

6. More insights into stellar atmospheres and stellar interiors will be coming from interferometry. Stay tuned!